473

3-Heteroaryl-Substituted Quinuclidin-3-ol and Quinuclidin-2-ene Derivatives as Muscarinic Antagonists. Synthesis and Structure–Activity Relationships

Björn M. Nilsson,[†] Staffan Sundquist,[‡] Gary Johansson,[†] Gunnar Nordvall,[†] Gunilla Glas,[‡] Lisbeth Nilvebrant,[‡] and Uli Hacksell*,[†]

Department of Organic Pharmaceutical Chemistry, Uppsala Biomedical Center, Uppsala University, Box 574, S-751 23 Uppsala, Sweden, and Department of Pharmacology, Pharmacia AB, S-751 82, Uppsala, Sweden
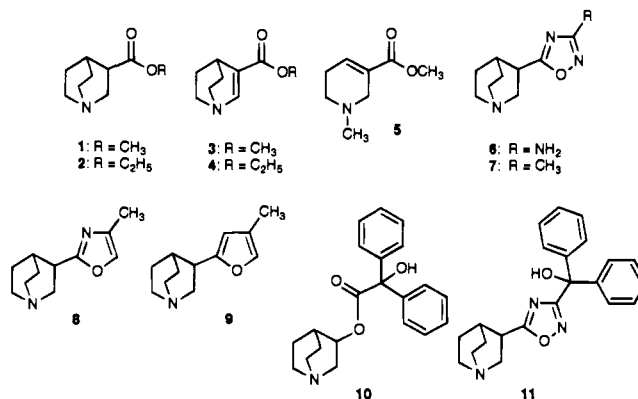
A number of 3-heteroaryl-substituted quinuclidin-3-ol and quinuclidin-2-ene derivatives have been prepared and evaluated for muscarinic and antimuscarinic properties. The affinities of the new compounds (**13**, **14**, **16–32**, and **36–52a,b**) were tested in homogenates of cerebral cortex, heart, parotid gland, and urinary bladder from guinea pigs using (−)-[^{3}H]-3-quinuclidinyl benzilate [(−)-[^{3}H]QNB] as the radioligand and in a functional assay using isolated guinea pig urinary bladder. The present compounds behaved as competitive muscarinic antagonists in the urinary bladder. The highest receptor binding affinity, K_i (cortex) = 9.6 nM, was observed for 3-(2-benzofuranyl)quinuclidin-2-ene (**31**). The corresponding 3-benzofuranyl (**36**) and 3-benzothienyl (**37**) homologues had about 3.5-fold lower affinity for cortical muscarinic receptors. All quinuclidin-3-ol derivatives (**14** and **16–25**) had lower binding affinities for the different muscarinic receptor subtypes than the corresponding quinuclidin-2-ene analogues when examined in the various tissue homogenates. In general, the new compounds showed low subtype selectivity. The structure–affinity relationships are discussed in terms of differences in proton basicity of the azabicyclic nitrogen and differences in geometric, conformational, and/or electronic properties of the compounds. The cortical antimuscarinic potency is also related to the complementarity of the compounds to the putative binding site of the muscarinic m1 receptor.

Introduction

Several series of muscarinic agonists with five- or six-membered heteroaromatic rings connected to a mono- or bicyclic ring system such as 1,2,5,6-tetrahydropyridine, quinuclidine, or 1-azanorbornane have been described.[1,2] The major objective of these investigations was to identify new muscarinic agonists with potential utility in the treatment of senile dementia of the Alzheimer type.[1] 1,2,4-Oxadiazole,[1] 1,2,4-thiadiazole,[3] tetrazole,[4] and pyrazine[5] moieties were found to be suitable stable bioisosteres for the ester group in the muscarinic agonists methyl quinuclidine-3-carboxylate (**1**)[6] and arecoline (**5**). The 1,2,4-oxadiazole derivatives **6** and **7** were among the most potent and efficacious compounds in these series.[1a] High affinity and efficacy required two hydrogen bond acceptor sites in exact locations of the heteroaromatic ring.[1] In addition, binding to the high-affinity state (the agonist binding site) of the receptor correlated with the magnitude of the negative electrostatic potential adjacent to these two locations.[1] Thus, a systematic removal of the heteroatoms in the 1,2,4-oxadiazole moiety of **7**, to give the oxazole (**8**) and furan (**9**) analogues, resulted in diminished affinity and efficacy at the muscarinic receptor.[1a]

Introduction of substituents larger than methyl in the 3-position of the oxadiazole ring of **7** produced compounds with weak partial agonist (ethyl) or antagonist (benzyl) profiles.[1a] Similarly, addition of a methylene group to the ester group of **1**, to give ethyl ester **2**, changed the activity from agonism to competitive antagonism at ileal muscarinic receptors.[6] In the oxadia-

zole series, the QNB (3-quinuclidinyl benzilate; **10**) analogue **11** proved to be a very potent muscarinic antagonist, displaying about 8-fold higher affinity to cortical muscarinic receptors than atropine.[1a]

It is noteworthy that introduction of a double bond between C2 and C3 in the quinuclidine ring of **7**, affording **12**, was detrimental to efficacy and affinity, since the binding to the high-affinity and low-affinity (the antagonist binding site) states of the receptor was lowered 444-fold and 34-fold, respectively.[1a,7] Additional muscarinic quinuclidin-2-ene derivatives have been reported in a patent application.[8]
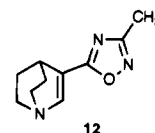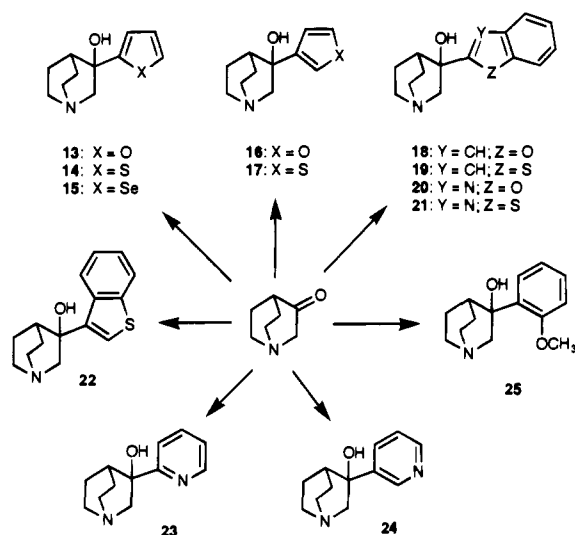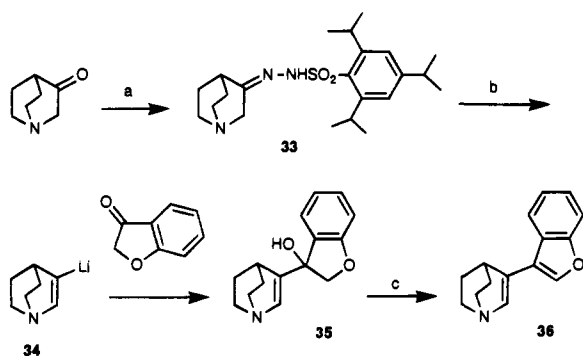

Hydrogen-bonding interactions between the muscarinic receptor and the heteroaromatic ring of the ligand
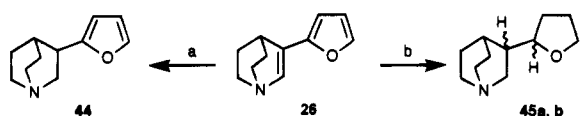
---

† Uppsala University.
‡ Pharmacia AB.

Scheme 1

13: X = O
14: X = S
15: X = Se

16: X = O
17: X = S

18: Y = CH; Z = O
19: Y = CH; Z = S
20: Y = N; Z = O
21: Y = N; Z = S

22

25

23

24

Scheme 2^a

33

34

35

36

^{a} Reagents: (a) 2,4,6-triisopropylbenzenesulfonyl hydrazide, ether; (b) n-BuLi (2 equiv), THF, 0 °C; (c) HCOOH, 100 °C.
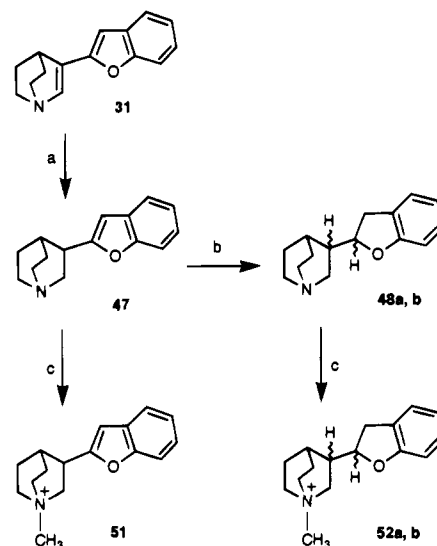
Scheme 3^a

44

26

45a, b

^{a} Reagents: (a) H$_2$, 10% Pd/C, THF; (b) H$_2$, 5% Rh on alumina, THF.

seem to be of minor importance, and instead size and lipophilicity appear to be major determinants for binding to the low-affinity state.[1a] Therefore, we have prepared some heterocyclic 3-substituted quinuclidin-3-ol and quinuclidin-2-ene derivatives to further investigate the structure—affinity relationships for quinuclidine-based muscarinic antagonists.[9] The compounds were investigated for their ability to displace (−)-[^{3}H]-3-quinuclidinyl benzilate [(−)-[^{3}H]QNB] from muscarinic receptors in cerebral cortex, heart, parotid gland, and urinary bladder from guinea pigs. In addition, the antimuscarinic potencies were evaluated in a functional assay on the isolated guinea pig urinary bladder.

Chemistry

The syntheses of the compounds are outlined in Schemes 1—4. Physical data of intermediate **15** and the test compounds (**13, 14, 16—32,** and **36—52a,b**) are presented in Table 1. The syntheses of **13**,[1a] **16**,[10] **23**,[11] **24**,[11b] **25**,[12] **26**,[1a] **40**,[11] **41**,[11b] and **42**[12] have been described previously. However, no pharmacological data on muscarinic properties were reported for any of these compounds.

Scheme 4^a

31

47

48a, b

51

52a, b

^{a} Reagents: (a) H$_2$, 10% Pd/C, THF; (b) H$_2$, 10% Pd/C, HOAc; (c) MeI, acetone or ether.

3-Aryl-3-hydroxyquinuclidines **13—25** (Scheme 1) were synthesized by addition of quinuclidin-3-one to the appropriate aryllithium compound in THF or ether. Direct metalation (method Ia)[13] or metal—halogen exchange (method Ib)[14] was used to generate the aryllithium compounds. Dehydration of **13—19, 22,** and **25** to the corresponding quinuclidin-2-ene analogues (**26—32, 37,** and **42**) was readily accomplished by heating a solution of the hydroxy compound in concentrated formic acid (method IIa). However, benzoxazole **20**, benzothiazole **21**, and the pyridine derivatives **23** and **24** were resistant to dehydration using formic acid. Instead, these derivatives were dehydrated under harsher conditions; treatment with methanesulfonic acid at 180—200 °C (method IIb) produced the corresponding quinuclidin-2-ene analogues **38—41**.

An alternative to the above approach was sought for the preparation of 3-(3-benzofuranyl)quinuclidin-2-ene (**36**), since generation of 3-benzofuranyllithium and subsequent reactions with different electrophiles have most frequently resulted in low yields of the expected addition products due to competitive ring opening of 3-benzofuranyllithium.[15] The synthetic strategy described in Scheme 2 was chosen for the preparation of **36**. Thus, treatment of the ((triisopropylphenyl)sulfonyl)hydrazone **33** with 2 equiv of n-BuLi (the Shapiro reaction)[16] generated 3-lithioquinuclidin-2-ene (**34**),[17] which upon reaction with the commercially available 2,3-dihydrobenzofuran-3-one gave **35**. Dehydration of **35** to **36** was accomplished by heating a solution of **35** in formic acid.

3-(2-Hydroxyphenyl)quinuclidin-2-ene (**43**) could not readily be obtained by demethylation of methoxy derivative **42** by use of 47% aqueous hydrogen bromide under reflux since several byproducts were formed (TLC).[18] Instead, 2-bromophenol was treated with 2 equiv of n-BuLi[19] and subsequently with quinuclidin-3-one. The crude product formed was directly dehydrated by use of formic acid to provide a low overall yield (4%) of **43**.

The quinuclidine analogues **44**[20] (Scheme 3) and **47** (Scheme 4) were obtained from the 2,3-unsaturated **26** and **31**, respectively, by hydrogenation over palladium on carbon in THF at atmospheric pressure (method III).

Table 1. Yields and Physical Data of Compounds Tested

| compd	method[a]	% yield	mp, °C	recryst solvent[b]	formula
13	Ia	73	176.5–177.5	A	$C_{11}H_{15}NO_2 \cdot C_4H_4O_4$
14	Ia	89	208–210	B	$C_{11}H_{15}NOS \cdot 0.5C_4H_4O_4$
15[c]	Ia	81[d]	210–212.5	C	$C_{11}H_{15}NOSe$
16	Ib	49	207–209	B	$C_{11}H_{15}NO_2 \cdot 0.5C_4H_4O_4$
17	Ib	50	219–220	B	$C_{11}H_{15}NOS \cdot 0.5C_4H_4O_4$
18	Ia	79	203–204	B	$C_{15}H_{17}NO_2 \cdot 0.5C_4H_4O_4$
19	Ia	66[e]	219–220	B	$C_{15}H_{17}NOS \cdot HCl$
20	Ia	45[f]	248–249	B	$C_{14}H_{16}N_2O_2 \cdot 0.5(COOH)_2$
21	Ia	95	233–235	B	$C_{14}H_{16}N_2OS \cdot HCl$
22	Ib	82[d]	216–218	D	$C_{15}H_{17}NOS \cdot HCl \cdot 0.25H_2O$
23	Ib	57[d]	208–215	B	$C_{12}H_{16}N_2O \cdot 2HCl$
24	Ib	46[d]	219–225	D	$C_{12}H_{16}N_2O \cdot 2HCl$
25	Ia	53	118–119	E	$C_{14}H_{19}NO_2 \cdot (COOH)_2$
26	IIa	91	144–145.5	B	$C_{11}H_{13}NO \cdot (COOH)_2$
27	IIa	94	180–182	B	$C_{11}H_{13}NS \cdot 0.5C_4H_4O_4$
28	IIa	95	137–138	D	$C_{11}H_{13}NSe \cdot (COOH)_2$
29	IIa	96	181.5–183.5	B	$C_{11}H_{13}NO \cdot 0.5C_4H_4O_4$
30	IIa	96	208–210	B	$C_{11}H_{13}NS \cdot 0.5C_4H_4O_4$
31	IIa	92	216–217	B	$C_{15}H_{15}NO \cdot 0.5C_4H_4O_4$
32	IIa	80	250–252	B	$C_{15}H_{15}NS \cdot HCl$
36	g	24[h]	113–114	B	$C_{15}H_{15}NO \cdot (COOH)_2 \cdot ^1/_3H_2O$
37	IIa	84	185–186	D	$C_{15}H_{15}NS \cdot HCl$
38	IIb	56	199.5–201.5	B	$C_{14}H_{14}N_2O \cdot HCl$
39	IIb	66	196.5–198.5	D	$C_{14}H_{14}N_2S \cdot HCl$
40	IIb	48	72–74	F	$C_{12}H_{14}N_2$
41	IIb	49	239–245	D	$C_{12}H_{14}N_2 \cdot 2HCl$
42	IIa	96	176–177.5	D	$C_{14}H_{17}NO \cdot HCl$
43	IIa	4[i]	169–170	B	$C_{13}H_{15}NO \cdot (COOH)_2$
44	III	74[j]	162–163	B	$C_{11}H_{15}NO \cdot C_4H_4O_4$
45a	g	31	154–155	E	$C_{11}H_{19}NO \cdot C_4H_4O_4$
45b	g	31	148.5–149.5	B	$C_{11}H_{19}NO \cdot C_4H_4O_4$
46[c]	g	92	159–161	G	$C_{12}H_{21}Cl_2NO$
47	III	87	172–173	B	$C_{15}H_{17}NO \cdot C_4H_4O_4$
48a	g	70	203.5–204.5	B	$C_{15}H_{19}NO \cdot 0.5C_4H_4O_4$
48b	g	56	166–167	B	$C_{15}H_{19}NO \cdot C_4H_4O_4$
49	IV	86	200–202	H	$C_{16}H_{20}INO_2$
50	IV[k]	63	182–183	D	$C_{16}H_{18}INO$
51	IV[k]	52	150–152	I	$C_{16}H_{20}INO$
52a	IV	96	205–207 dec	J	$C_{16}H_{22}INO$
52b	IV	91	244–246	J	$C_{16}H_{22}INO$

[a] Letters refer to methods of preparation in the Experimental Section. [b] A, acetonitrile–ethanol–ether; B, acetone–methanol–ether; C, ethyl acetate–methanol–n-hexane; D, methanol–ether; E, acetone–ether; F, n-hexane; G, trituration with ether; H, trituration with acetone; I, methanol–ethyl acetate; J, methanol–acetone. [c] Not tested. [d] No chromatography of the free base on alumina; the crude product was triturated with n-hexane several times prior to formation of the salt. [e] 3-Bromobenzothiophene, used for generation of the corresponding 3-lithio compound, was prepared according to ref 72. The crude product was purified by chromatography on silica using petroleum ether as eluant. [1]H[73] and ^{13}C NMR[74] data were in accordance with those previously reported. [f] Competitive ring opening may be a side reaction in the lithiation of benzoxazole, see ref 75. [g] See the Experimental Section. [h] Overall yield from 33. [i] Overall yield from quinuclidin-3-one. [j] The free base of 44 was purified by column chromatography on silica using ammonia-saturated chloroform followed by ammonia-saturated chloroform/methanol (99:1). [k] Acetone was changed into ether as the solvent.

Exchange of the catalyst in the hydrogenation of 26 for rhodium on alumina[21] furnished 3-(2-tetrahydrofuranyl)quinuclidine as an approximate 1:1 mixture of diastereomers (45a and 45b; Scheme 3) according to capillary GLC analysis. The less polar isomer (by GLC and TLC) is denoted 45a. The diastereomers were separated (de ≥99% for both 45a and 45b) by column chromatography on alumina.[22] In contrast, the diastereomers of 3-(2,3-dihydrobenzofuran-2-yl)quinuclidine (48a and 48b; Scheme 4)[22] could not be obtained by hydrogenation of 31 using rhodium on alumina since we were only able to isolate 47 from the reaction mixture. However, 48a and 48b were obtained in a 1:1 ratio (GLC) by hydrogenating 47 over palladium on carbon at atmospheric pressure using glacial acetic acid[23] as the solvent. The diastereomers were separated [de ≥99% for both 48a (shortest GLC retention time) and 48b] by chromatography on silica. Attempts to prepare 48a/48b from 47 using ionic hydrogenation[24] (triethylsilane, trifluoroacetic acid, 50 °C) was less useful since only a low conversion to 48a/48b (TLC) was achieved.

The quaternary ammonium salts 49–52a,b were

prepared by treatment of the corresponding tertiary amines 18, 31, and 47–48a,b with iodomethane (method IV). In the ^{13}C NMR spectra of CD₃OD solutions of 50–52a,b, signals due to C2, C4, C6, and C7 in the quinuclidine ring and the N-methyl group appeared as triplets. This phenomenon seems to emerge from ^{13}C, ^{14}N couplings [^1J (^{13}C, ^{14}N) = 3–5 Hz and ^3J (^{13}C, ^{14}N) = 4–5 Hz] and has previously been observed in rigid tetraalkylammonium compounds such as quinuclidine methiodide.[25]

Basicity of the Azabicyclic Nitrogen. The receptor binding assays were performed at 25 °C and pH 7.4. Most likely the heteroaryl-substituted quinuclidine and quinuclidin-2-ene derivatives interact with the muscarinic receptor binding sites in the protonated state.[26] Hence, the pK_a of the compound may influence the measured affinity by determining the fraction that is protonated at a certain pH. Therefore, we determined the pK_a values of some selected compounds that displayed differences in affinity: The quinuclidin-3-ol derivatives substituted with a 2-furanyl (13) or a 2-benzofuranyl (18) ring had pK_a values of 9.06 and 8.84, respectively. 3-(2-Furanyl)quinuclidine (44) and
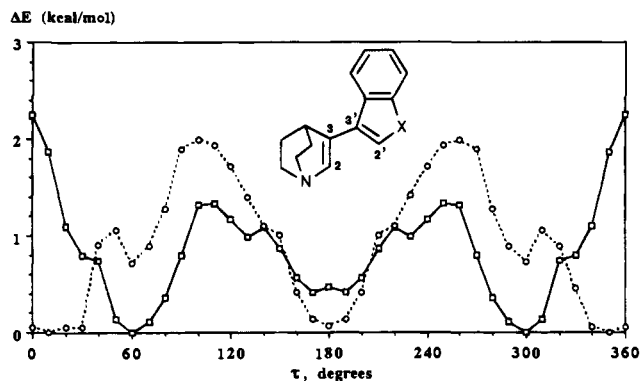
Figure 1. The PM3-derived conformational energy curves for rotation about the acyclic torsional angle τ (C2−C3−C3'−C2') in **36** (X = O, dotted line) and **37** (X = S; solid line).
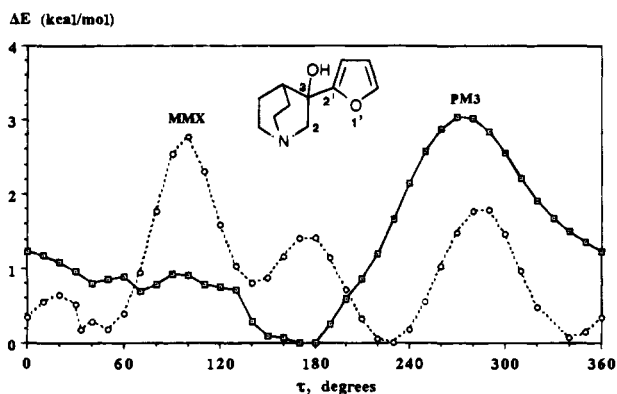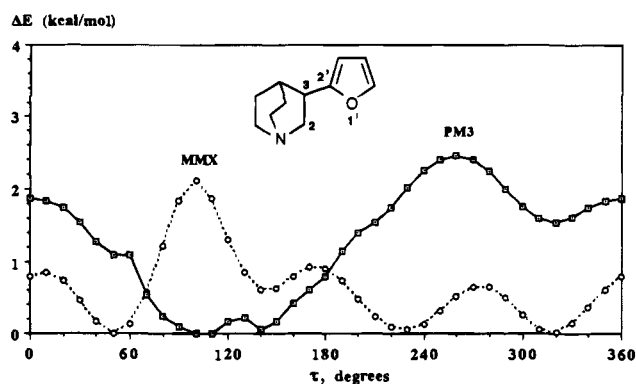

Figure 2. Conformational energy curves for rotation about the acyclic torsional angle τ (C2−C3−C2'−O) in **13**. The dihedral angle values refer to the S configuration.

3-(2-furanyl)quinuclidin-2-ene (**26**) had pK_a values of 10.03 and 8.92, respectively.[27] The pK_a values of the corresponding benzo homologues **47** and **31** could not be determined due to the low water solubility of the bases. 3-(2-Benzoxazolyl)quinuclidin-2-ene (**38**) and its corresponding benzothiazole derivative **39** had pK_a values of 7.23 and ~7.4,[28] respectively.

Molecular Modeling. Conformational Analysis.
Two objectives of the present study were to relate the differences in affinities to geometric, conformational, and/or electronic properties of the novel antagonists and to explore possible binding interactions with the muscarinic receptor. Therefore, we studied the conformational profiles of some selected compounds from the different structural classes; dihedral driver calculations were performed by exploring the acyclic torsional angle τ (see Figures 1−3) using the semiempirical molecular orbital methods AM1[29] and PM3,[30] respectively, and by molecular mechanics calculations using the MMX-89.0[31] force field (for details, see the Experimental Section). All calculations were done on the unprotonated amines. The torsional angle was rotated in 10-deg increments (0−360°) and held constant while the remaining structure was geometry optimized. The AM1 and PM3 calculations performed on the 2-furanyl- (**26**), 2-benzo-furanyl- (**31**), 2-benzothienyl- (**32**),[32] and 2-benzoxazolyl-substituted (**38**) quinuclidin-2-ene analogues, respectively, indicated that coplanar conformations (two equally populated rotameric forms) are favored.[33] However, there was essentially free rotation about τ since only low barriers to rotation were observed for **26**, **31** and **38** (2.7 kcal/mol, AM1; 1.8 kcal/mol, PM3).[34] The

Figure 3. Conformational energy curves for rotation about the acyclic torsional angle τ (C2−C3−C2'−O) in **44**. The dihedral angle values refer to the R configuration.

rotational barrier for **32** was even lower (0.9 kcal/mol; PM3).

PM3 calculations performed on **36** revealed preferences for the coplanar conformations with a rotational barrier of 2 kcal/mol (Figure 1). However, the corresponding 3-benzothienyl derivative **37** displays global minimum-energy conformations at τ = 60 and 300° (PM3). The coplanar conformations were 2.2 kcal/mol (τ = 0°) and 0.5 kcal/mol (τ = 180°) higher in energy (Figure 1). Apparently, **37** has a global energy maximum at τ = 0° whereas this conformation represents a global minimum-energy conformation of **36**. The rotamer with τ = 0° is probably disfavored in **37** due to repulsive interactions between, in particular, the C4-hydrogens in both ring systems. The interatomic distance between the interacting hydrogens in **37** is 1.64 Å whereas the corresponding distance in **36** is 1.85 Å. This is a consequence of the different geometries of the five-membered heterocyclic rings.

Molecular mechanics and semiempirical PM3 calculations were performed on alcohol **13** (Figure 2) and its corresponding 3-deoxy analogue **44** (Figure 3). From the MMX calculations on **13** it was observed that when τ adopts values (80−120°) favoring formation of an intramolecular hydrogen bond between the furan oxygen and the hydroxyl proton, the energy reaches a maximum due to the proximity between the endo proton on C5 and the proton on C3 in the furan ring (at τ = 100° the interatomic distance is 2.0 Å). This maximum was also observed in the MMX calculations of **44**. On the other hand, the PM3 calculations performed on the same compounds produced conformers with highest energy at τ about 270° (see Figures 2 and 3) due to the proximity between the proton (**44**) or oxygen atom (**13**) on C3, respectively, and the proton on C3 in the furan ring.

UV Spectroscopy.[35] To gain insight into the conformational behavior of the quinuclidin-2-ene derivatives also in solution, we investigated UV-spectral characteristics of selected compounds (Table 2) and compared the results with the corresponding molecular modeling data. For example, a predominance of coplanar conformations of **26** in solution was indicated by the bathochromic shift and the increase in λ_{max} in going from **44** to **26**.

Electrostatic Potential Energy Calculations. To investigate the influence of electronic properties on the affinity, we calculated the electrostatic potential of quinuclidin-2-ene analogues **31**, **32**, **38**, and **39**. The protonated forms of both coplanar rotamers of each
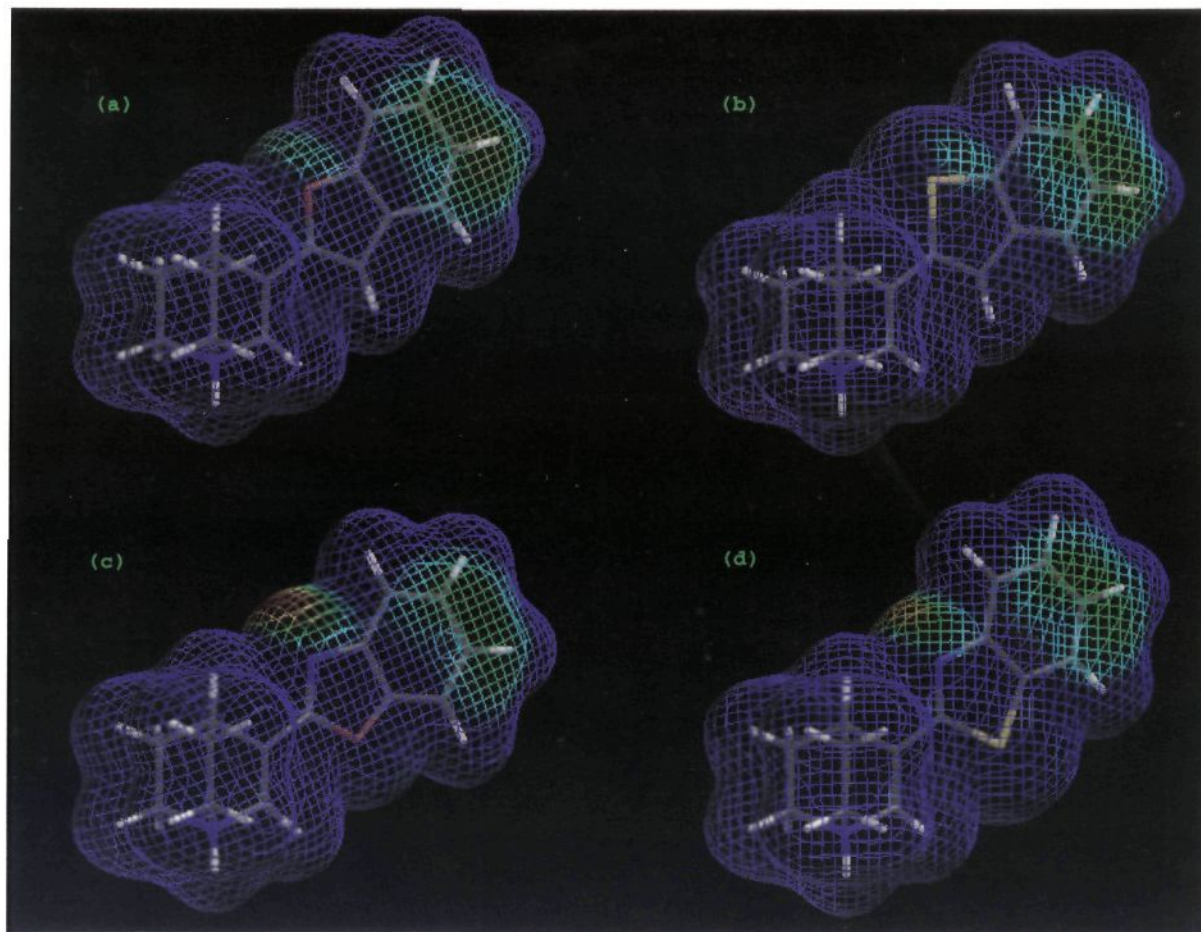
Figure 4. Electrostatic potentials, color coded according to magnitude and displayed on the electron density surface of (a) **31**, (b) **32**, (c) **38**, and (d) **39**. Red represents the lowest and blue represents the highest electrostatic potential. For clarity, the range of the electrostatic potential is restricted to the interval 25–50 kcal/mol.

Table 2. UV Spectral Data of Some Furan (**13**, **26**, and **44**) and Benzofuran Analogues (**18**, **31**, and **47**)[a]

compd	λ_{max}, nm (log ϵ)
13	213 (3.97), 217 (3.97)
18	248 (4.19), 278 (3.59), 285 (3.59)
26	268 (4.23)
31	288 (4.40), 294 (4.40), 306 (4.39)
44	217 (3.98)
47	248 (4.24), 278 (3.64), 285 (3.63)

[a] Spectra were recorded on the free base in methanol.

compound were geometry optimized using PM3. Electrostatic properties were calculated using the 6-31G* basis set,[36] color coded according to magnitude, and displayed on the electron density surface of the compounds. The examined compounds have an electrostatic potential minimum located in the benzene part of the heterocycle (Figure 4). In addition, **38** and, to a lesser degree, **39** have large electrostatic potential minima located near the nitrogen atom in the heteroaromatic ring.

Pharmacological Results

Receptor binding affinities (expressed as K_i values; Table 3) for muscarinic receptor subtypes[37] in cortex (M_1), heart (M_2), parotid gland (M_3), and urinary bladder were determined indirectly for each compound by competition experiments with (−)-[³H]QNB.[38–41] The antimuscarinic potencies (expressed as K_B values; Table 3) were evaluated by functional *in vitro* studies on the

isolated guinea pig urinary bladder, using carbachol as the standard agonist. In the presence of antagonist, the concentration–response curves to carbachol were shifted in parallel toward higher concentrations, but the maximal responses remained unaffected. Thus, the inhibition seemed to be competitive since it could always be overcome by an increase in the carbachol concentration. None of the compounds in the present study exhibited any muscarinic agonist activity in the isolated bladder when tested in concentrations of 10–1000 μM. For comparison, reference data for **10** (racemic QNB), the M_1 selective antagonist pirenzepine,[42] and the M_2 selective antagonist AF-DX 116[43] are included in Table 3.

The alcohols **14** and **16–25**[44] invariably had lower affinities for all receptor subtypes studied than their corresponding 3-deoxyquinuclidine and quinuclidin-2-ene congeners (i.e., the rank order was **31** > **47** > **18**).

In general, there was a good agreement between receptor binding data (K_i) and functional data (K_B) in the urinary bladder since the same rank order of potency was noted for all receptor subtypes; i.e., −log K_i for each receptor subtype was plotted versus −log K_B for the alcohols (**14** and **16–25**) and the quinuclidin-2-enes (**27**, **29–32** and **37–42**), respectively. This produced regression lines with r^2 ranging from 0.79 to 0.90.

The most potent muscarinic antagonist in this series, the benzofuran analogue **31**, displayed about 188-fold lower affinity than **10** for cortical muscarinic receptors.

Table 3. Affinities (K_i) for Muscarinic Receptors, Determined by Competition Experiments with $(-)$-[^{3}H]QNB and Functional in Vitro Data (K_B), Determined on Isolated Urinary Bladder Strips from Guinea Pig vs Carbachol[a]

compd	R	general structure	K_i, nM cerebral cortex (M$_1$)	heart (M$_2$)	parotid gland (M$_3$)	urinary bladder	K_B, nM urinary bladder
13		A	30000 ± 1000	b	b	b	b
14		A	11600 ± 400	>18000	48000 ± 3000	45000 ± 300	40000 ± 9000
16		A	>15000	>53000	>53000	>58000	86500 ± 500
17		A	9200 ± 5	>18000	37000 ± 7000	>38000	84000 ± 17000
18		A	810 ± 10	2700 ± 500	4400 ± 90	6900 ± 20	710 ± 40
19		A	1100 ± 100	4200 ± 500	5400 ± 500	8600 ± 1100	3700 ± 500
20		A	1800 ± 200	9200 ± 1600	8400 ± 1000	19000 ± 1000	3900 ± 1000
21		A	1200 ± 200	3000 ± 400	3800 ± 200	8100 ± 800	4200 ± 7000
22		A	820 ± 100	2200 ± 100	2700 ± 500	5400 ± 900	4300 ± 800
23		A	10000 ± 2000	20000 ± 1000	38000 ± 2000	28000 ± 6000	28000 ± 5000
24		A	14900 ± 200	27000 ± 5000	67000 ± 17000	42700 ± 600	80000 ± 12000
25		A	7400 ± 800	15900 ± 100	29900 ± 700	28000 ± 2000	33000 ± 21000
26		B	300 ± 70	390 ± 60	1100 ± 90	850 ± 130	550 ± 30
27		B	290 ± 10	620 ± 110	1200 ± 200	1500 ± 300	1100 ± 200
28		B	410 ± 10	990 ± 190	1100 ± 200	b	b
29		B	1500 ± 20	1700 ± 100	4900 ± 40	4300 ± 900	3400 ± 100
30		B	710 ± 20	1700 ± 60	2600 ± 20	3700 ± 700	2010 ± 200

Table 3. (Continued)
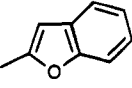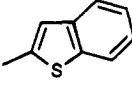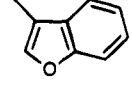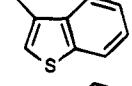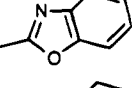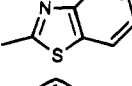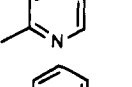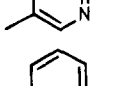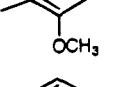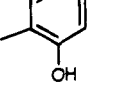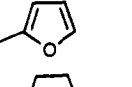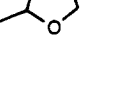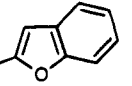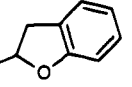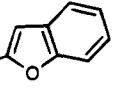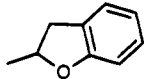
compd	R	general structure	K_i, nM cerebral cortex (M_1)	heart (M_2)	parotid gland (M_3)	urinary bladder	K_B, nM urinary bladder
31		B	9.6 ± 0.1	31 ± 4	59 ± 4	67 ± 15	33 ± 5
32		B	81 ± 2	270 ± 30	420 ± 3	550 ± 130	660 ± 150
36		B	34 ± 1	99 ± 14	160 ± 60	120 ± 10	b
37		B	37 ± 9	96 ± 9	110 ± 0.3	240 ± 60	170 ± 50
38		B	100 ± 6	400 ± 60	720 ± 160	580 ± 80	190 ± 40
39		B	170 ± 5	600 ± 50	1100 ± 200	760 ± 130	810 ± 80
40		B	1200 ± 300	1900 ± 20	4000 ± 500	3700 ± 500	1800 ± 300
41		B	2200 ± 600	2800 ± 30	5900 ± 30	6100 ± 300	3500 ± 200
42		B	220 ± 20	410 ± 20	740 ± 20	870 ± 90	670[c]
43		B	360 ± 70	330 ± 30	1400 ± 40	920 ± 240	2400 ± 500
44		C	540[c]	1500 ± 400	3100 ± 1300	2400 ± 800	2700 ± 100
45a		C	8100 ± 700	>20000	24000 ± 1000	>35000	22000 ± 5000
45b		C	2200 ± 500	5000 ± 1500	13000 ± 300	11000 ± 1000	6600 ± 1600
47		C	57 ± 4	200 ± 4	240 ± 30	310 ± 120	230 ± 90
48a		C	440 ± 10	1500 ± 300	2500 ± 300	5000 ± 600	1100 ± 300
48b		C	59 ± 11	160 ± 8	340 ± 20	410 ± 20	200 ± 70
49		D	3800 ± 700	5500 ± 100	16000 ± 3000	20000 ± 3000	b
50		E	360 ± 20	460 ± 20	1300 ± 30	600 ± 2	b
51		F	520 ± 30	1100 ± 100	2200 ± 200	2000 ± 80	b

Table 3. (Continued)

compd	R	general structure	K_i, nM cerebral cortex (M_1)	heart (M_2)	parotid gland (M_3)	urinary bladder	K_B, nM urinary bladder
52a		F	1700 ± 7	2600 ± 30	7500 ± 900	5400 ± 500	b
52b		F	1100 ± 30	1300 ± 100	5700 ± 700	3800 ± 600	b
(±)QNB; 10			0.051 ± 0.03[d]	0.045 ± 0.03[d]	0.24 ± 0.01[e]	0.20 ± 0.02[e]	
pirenzepine			14 ± 1[d]	270 ± 20[d]	110 ± 10[e]	530 ± 60[e]	
AF-DX 116			210 ± 20[f]	48 ± 5[f]	1500 ± 100[f]	150 ± 10[f]	

[a] Values are means ± SEM of two to three experiments performed in triplicate. [b] Not determined. [c] Value derived from a single determination. [d] Value is from ref 40. [e] Value is from ref 41. [f] Value is from ref 76.

Replacement of the 2-benzofuranyl moiety of **31** with a 2-benzothienyl, 2-benzoxazolyl, or a 2-benzothiazolyl moiety produced analogues (**32, 38,** and **39,** respectively) with about 8-, 10-, and 18-fold lower M_1 receptor binding affinities.

A shift in the position of the oxygen and sulfur atoms in **26** and **27,** to give the 3-substituted furan (**29**) and thiophene (**30**) analogues, decreased the affinity at each of the receptor subtypes by about 6-fold (**29**) and 2.5-fold (**30**). Replacement of the five-membered heterocycles (i.e., **26−28**) with a 2- or 3-pyridyl substituent (**40** and **41**) resulted in a drop in affinity (about 5−9-fold). However, the 2-methoxyphenyl- (**42**) and 2-hydroxyphenyl-substituted (**43**) analogues retained similar affinities as **26−28** at each of the muscarinic receptor subtypes.

In general, the new antimuscarinic compounds exhibited low subtype selectivity since the majority of the studied antagonists displayed less than 7-fold selectivity for any of the muscarinic receptor subtypes. A slightly higher selectivity was found for benzoxazole analogue **20** and dihydrobenzofuran derivative **48a**. The selectivity ratio for these compounds, which exhibited modest antimuscarinic potencies, was about 11-fold in favor of M_1 receptors in the cortex versus muscarinic receptors in the urinary bladder. By comparison, pirenzepine shows approximately 38-fold higher affinity for M_1 receptors in the cortex than for muscarinic receptors in the urinary bladder.

Discussion

Molecular properties such as proton affinity and electronic, geometric, and conformational factors may affect the mode of binding and the affinity of the present quinuclidine and quinuclidin-2-ene derivatives to the muscarinic receptors. Hence, we have studied these properties in some detail in order to find clues to the observed affinities within the present series of compounds. Because of the low subtype selectivity, we have chosen to use the affinity for cortical muscarinic receptors in most comparisons.

Differences in Basicity of the Azabicyclic Nitrogen. It is apparent that the observed affinity differences between the alcohols (**13, 14,** and **16−25**) and the corresponding quinuclidin-2-enes (**26, 27, 29−32,** and **37−42**) are unrelated to their proton affinities since **13** and **26** had similar pK_a values. On the other hand, differences in basicity may account for part of the 10-fold lower affinity of benzoxazole **38** as compared to the benzofuran homologue **31,** since their pK_a values would appear to differ with more than one pK_a unit (compare above); at pH 7.4, only about 40% of **38** would be protonated whereas **31** should be protonated to about 90%, based on the extrapolation that the pK_a value of **31** would be about 8.5.

Geometric, Conformational, and Electronic Factors. The 56- and 14-fold lower affinities of alcohols **13** and **18** compared to their 3-deoxy analogues **44** and **47,** respectively, are probably unrelated to conformational factors since **13, 18, 44,** and **47** display similar conformational preferences about τ according to molecular mechanics calculations and semiempirical molecular orbital calculations (PM3), respectively (see Figures 2 and 3).[45]

Introduction of a double bond in **44** and **47,** to give **26** and **31,** increased affinity by about 2- and 6-fold, respectively. This contrasts with the observation made in the oxadiazole series where the 2,3-dehydro analogue of agonist **7** (i.e., **12**) had 34-fold lower affinity for the low-affinity state of the receptor than the parent compound (*vide supra*). This suggests that the 2,3-dehydro analogues included in this series bind to the receptor in a manner different from that of **12**.

The results from the semiempirical molecular orbital calculations indicate that the conformational preferences for the quinuclidin-2-ene derivatives **26, 27, 29,** and **30** about the acyclic torsional angle τ are similar. The similar affinity displayed by **26−28**[46] on one hand and **29** and **30** on the other hand indicate that aromatic $\pi-\pi$ interactions[47] between the heteroaromatic ring and an aromatic side chain in the receptor may be of importance.[48] Compounds **26−30** may also form a weak
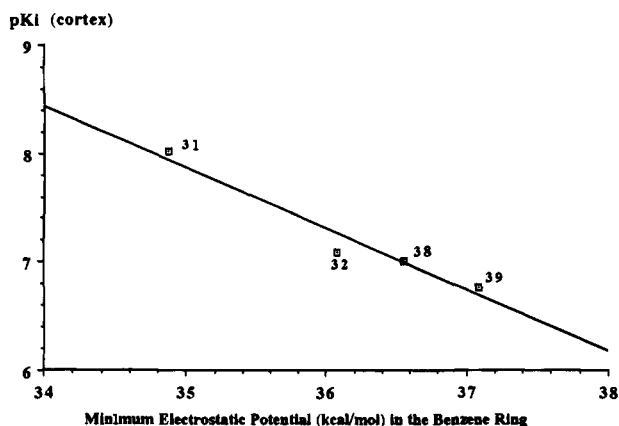
Figure 5. Relationship between receptor binding affinities ($-\log K_i$, M) at cortical muscarinic receptors of **31, 32, 38,** and **39** and the magnitude of the negative electrostatic potential in the benzene moiety. The regression line is described by pK_i (cortex) = -0.568(minimum electrostatic potential in the benzene ring) + 27.745 ($r^2 = 0.95$).

hydrogen bond with the receptor via the heteroatom or the π electron system of the heteroaromatic ring.[49-51]

The increase (50- and 20-fold, respectively) in affinity when additional steric bulk was introduced into the 3-furanyl (**29**) and 3-thienyl (**30**) derivatives, to give the almost equipotent benzo-fused homologues **36** and **37**, respectively, suggests increased hydrophobic binding or additional aromatic $\pi-\pi$ interactions between **36** and **37** and the receptor site. On the other hand, the increase in affinity (24- and 4-fold, respectively) on going from 2-furanyl (**26**) and 2-thienyl (**27**) to their benzo homologues **31** and **32**, respectively, resulted in a 8-fold higher affinity for benzofuran **31** relative to benzothiophene **32**. This may imply that the latter compounds would bind to the receptor in an orientation and/or in a conformation which may be different from that of the almost equipotent **26** and **27**.[52] The PM3-optimized structures of **31** and **32** were compared by fitting the heavy atoms in the quinuclidinene ring. Due to the slightly different geometries in the heteroaromatic ring, the benzene moieties do not overlap perfectly. The lower affinity of **32** compared to **31** may thus also be related to steric factors.

Different relative locations in steric bulk presented by the benzene part of **31** and **32** on one hand and **36** and **37** on the other hand seem to be well-accommodated by the receptor since no gross differences in affinity were observed between these two pairs of compounds.

Assuming that the benzofuran oxygen in **31** participates in a stabilizing hydrogen bond interaction with the receptor, it is tempting to suggest that a switch in hydrogen bond acceptor site occurs from oxygen to nitrogen in the benzoxazole analogue **38** since the nitrogen atom has better hydrogen bond accepting potential than the oxygen atom.[53] Nevertheless, a 10-fold drop in affinity was observed for **38** relative to **31**. Therefore, the presence of a hydrogen bond to the heteroatom is less plausible. The affinity difference between **31** and **38** is probably unrelated to conformational factors since **31** and **38** have similar conformational preferences about τ (AM1 and PM3).

There appears to be a good correlation ($r^2 = 0.95$) between the affinity of **31, 32, 38,** and **39** to muscarinic receptors in cortex (M_1) and the magnitude of the negative electrostatic potential in the benzene moiety (Figure 5). This area of negative potential may interact

favorably with receptor sites, e.g., in aromatic edge to face interactions with aromatic side chains[47] or in hydrogen bond interactions.

The drop in affinity when the quinuclidine nitrogen was quaternized by *N*-methylation of **18, 31, 47,** and **48a,b**, to give **49–52a,b**, agrees with observations made previously with other quinuclidines (e.g., **1**,[6] **2**,[6] and **6**[1a]), quinuclidin-2-enes (e.g., **3**[6] and **4**[6]), and the quaternary *N*-methyl analogue of **5**.[54] Thus, when a tertiary amino nitrogen is part of a ring, it appears that *N*-methylation sterically hinders the interaction with the receptor.[55]

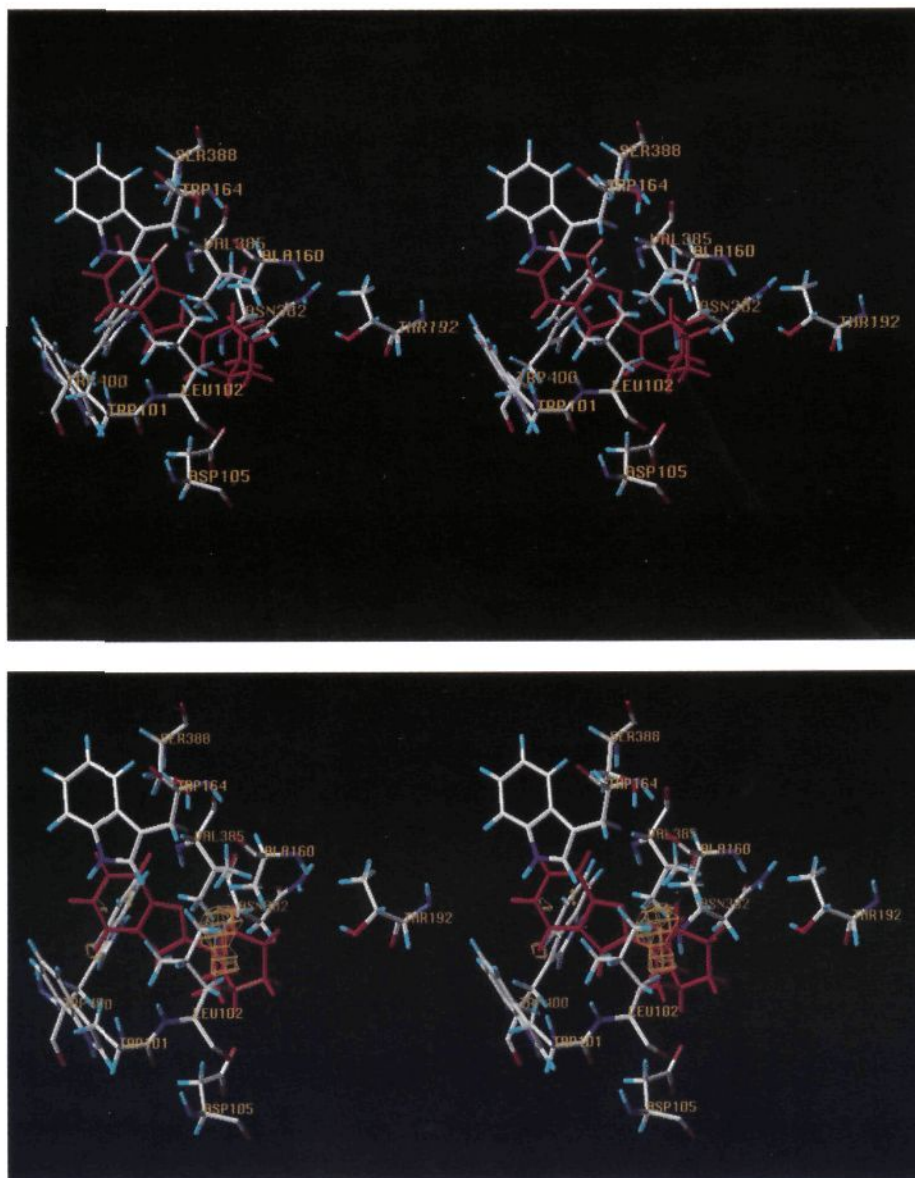**Interactions with a Muscarinic Receptor Model.** To study the possible receptor–ligand interactions in this series of quinuclidine-based antagonists, we used a homology-based binding site model of the muscarinic m1 receptor previously described by us.[56] The model is based on the presumed homology in three dimensional structure between bacteriorhodopsin and the G-protein coupled receptors and it rationalizes, in a qualitative way, the binding of a series of structurally different muscarinic agonists. A number of the present antagonists were docked into the binding site model. The docking was performed manually in Sybyl so that attractive interactions were optimized and repulsive interactions were minimized. In addition, side chain conformations were changed manually to minimize overlap between ligands and receptor. Coplanar conformations (PM3) of the quinuclidin-2-ene derivatives and conformations of the quinuclidin-3-ol derivatives with $\tau = 100°$ (PM3; see Figure 2) were used in the dockings.

A number of site-directed mutagenesis and chemical modification studies have been performed on the muscarinic receptors. Asp105 in the third transmembrane region (TM3) has been demonstrated to be of importance for both agonist and antagonist binding.[57] Chimeric receptors have also been constructed to study antagonist selectivity. These studies indicate that structurally different antagonists may interact in different ways with the receptor.[58]

Structure–activity relationship studies of a number of heteroaromatic muscarinic agonists indicate that two hydrogen bond acceptor sites in the appropriate positions on a five-membered heteroaromatic ring are of importance for agonist efficacy.[1a,c] This was also suggested by our previous study of the binding site model[56] since hydrogen bonds could form between Thr192 and Asn382 and the two nitrogens of a 1,2,4-oxadiazole ring in (3*R*,4*R*)-**53**.[59] The present five-membered heteroaromatic compounds lack at least one of these sites. Consequently, none of these compounds are agonists and, therefore, they interact differently with the receptor than the closely related quinuclidine-based agonists.

(3*R*, 4*R*)-**53**
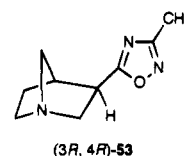
In the docking of the benzofuran derivative **31** to the binding site model of the m1 receptor, the protonated nitrogen forms a hydrogen bond reinforced ionic interaction[60] with Asp105. The quinuclidinene ring is located in an area of the receptor defined by Val102, Ala160, and Val385. This part of the receptor cavity is also occupied by the azabicyclic ring system of the potent

Figure 6. Stereorepresentation of the docking of **31** (top) and (*S*)-**18** (bottom) (ligands shown in red) into the muscarinic m1 receptor model. The benzofuran derivative **31** forms a reinforced ionic interaction with Asp105 and has an aromatic–aromatic interaction with Trp400. The low affinity of (*S*)-**18** is explained by a steric interaction between the ligand and the receptor. The van der Waals overlap between the hydroxyl group of (*S*)-**18** and the binding site is displayed in yellow.

agonist (3*R*,4*R*)-**53**.[56] The aromatic ring of the antagonist is, however, directed away from the agonist binding site. Thus, the benzofuran ring of **31** appears to bind to an area of the receptor model defined by Trp101 (TM3), Leu102 (TM3), Trp164 (TM4), and Trp400 (TM7). The indole ring of Trp400 forms an edge to face aromatic interaction with the benzenoid ring of **31** (Figure 6). This interaction would occur in the area of negative electrostatic potential identified by *ab initio* calculations.

The furan analogue **26**, which is significantly less potent than **31**, does not appear to bind optimally to the aromatic cavity due to its smaller size. The alcohol derivatives **13**, **14**, and **16**–**25** also show a significantly lower affinity than the corresponding quinuclidin-2-ene derivatives. Docking of both (*R*)- and (*S*)-**18** into the receptor model indicates that the lower affinity is related to steric interactions between the ligand and the receptor; the hydroxyl group of (*S*)-**18** interacts unfavor-

ably with Leu102 (Figure 6) and that of (*R*)-**18** with Val385.

Conclusions. In the present series of muscarinic antagonists, a benzo-fused five-membered heteroaromatic ring with one heteroatom attached to quinuclidin-2-ene in the 3-position (i.e., **31**, **32**, **36**, and **37**) provides the highest affinity. Thus, as seen from previous studies, muscarinic antagonists should have nonpolar moieties, such as phenyl groups, which are able to participate in hydrophobic binding.

The affinity difference between the quinuclidin-2-ene derivatives and the corresponding quinuclidin-3-ol analogues was tentatively rationalized in terms of a previously described m1 receptor model. In addition, the magnitude of the electrostatic potential minimum in the benzene part of the benzo-fused 2-heteroaryl analogues (i.e., **31**, **32**, **38**, and **39**) appears to correlate with M_1 receptor affinity. Therefore, further studies on substituted furans and benzofurans attached to quinuclidin-

2-ene could help in the design of new muscarinic antagonists with optimal binding to the muscarinic m1 receptor.

Experimental Section

Chemistry. General Comments. Reactions were carried out under nitrogen. Melting points were determined in open glass capillaries on a Thomas-Hoover apparatus. UV spectra were recorded on a Cecil 3000 spectrometer. IR spectra were recorded on a Perkin-Elmer 298 infrared spectrophotometer. ^{1}H and ^{13}C NMR[61] spectra were recorded on a JEOL FX 90Q spectrometer at 89.55 and 22.5 MHz, respectively, or on a JEOL JNM-EX 270 spectrometer at 270.2 and 67.9 MHz, respectively. ^{1}H and ^{13}C NMR spectra were referenced to internal tetramethylsilane. Dioxane (3.60 and 68.0 ppm, respectively) was used as internal reference for ^{1}H and ^{13}C NMR spectra recorded in D_2O. All spectra were in accordance with the assigned structures. Capillary GLC analyses were performed on a Carlo Erba 6000 Vega instrument equipped with a FID-40 flame ionization detector and a LDC Milton Roy CI-10B integrator; GLC column: DB-5 fused silica (30 m, i.d. = 0.32 mm); carrier Helium (50–80 kPa). Thin-layer chromatography was carried out on aluminum sheets precoated with silica gel 60 F_{254} (0.2 mm) or aluminum oxide 60 F_{254} neutral (type E) (E. Merck). Column chromatography was performed on silica using Kieselgel 60 (230–400 mesh), E. Merck, or on alumina using Aluminum oxide 90, E. Merck. Chromatographic spots were visualized by UV and/or I_2 vapor. The elemental analyses were performed by Mikro Kemi AB, Uppsala, Sweden, or Analytische Laboratorien, Gummersbach, Germany, and were within ±0.4% of the calculated values.

General Method Ia. 3-(2-Benzothiazolyl)quinuclidin-3-ol Hydrochloride (21). A solution of benzothiazole (3.68 g, 27.2 mmol) in ether (60 mL) was added dropwise to a stirred solution of *n*-butyllithium in hexane (1.3 M; 17 mL, 22.1 mmol) at −78 °C. After 10 min a solution of quinuclidin-3-one [2.63 g, 21.0 mmol; generated from the corresponding commercially available hydrochloride by alkalization (5 M aqueous sodium hydroxide), extraction with $CHCl_3$, drying (K_2CO_3), filtration, and concentration of the organic layer in vacuo] in ether (25 mL) was added. The external cooling was interrupted and the reaction mixture was stirred at room temperature for 64 h. A saturated aqueous ammonium chloride solution (20 mL) was added dropwise, and the mixture was diluted with 2.5 M aqueous hydrochloric acid (40 mL) and washed with ether (2 × 50 mL). The aqueous layer was alkalinized (pH ∼ 13) with 5 M aqueous sodium hydroxide. Product that precipitated from the alkaline mixture was collected after being triturated with ether. The aqueous layer was extracted with ether (6 × 200 mL). The combined organic layers were dried (K_2CO_3), filtered, and concentrated in vacuo. Column chromatography of the crude product on alumina using $CHCl_3$ followed by $CHCl_3/MeOH$ (95:5) as eluents yielded 5.18 g (95%) of the pure base which was converted into its hydrochloride salt and recrystallized. **21**: TLC R_f (free base on alumina) = 0.32 [$CHCl_3/MeOH$ (95:5)]; ^{1}H NMR (89.55 MHz, D_2O) δ 7.92–7.74 (m, 2 ArH's), 7.51–7.20 (m, 2 ArH's), 4.23 (app. d, J = 14.0 Hz, 2-CH), 3.49–3.00 (m, 2-CH, 6-CH_2, and 7-CH_2), 2.46–2.10 and 2.07–1.51 (each m, 2 H and 3 H, respectively, 4-CH, 5-CH_2, and 8-CH_2); ^{13}C NMR (22.5 MHz, D_2O) δ 177.70 (benzothiazole C2), 153.02 (benzothiazole C3a), 136.53 (benzothiazole C7a), 128.13, 127.48, 123.99, 123.81, 74.05 (C3), 59.29 (C2), 47.86 and 47.15 (C6 and C7), 33.94 (C4), 19.98 and 19.24 (C5 and C8). Anal. ($C_{14}H_{16}N_2OS$·HCl) C, H, N.

General Method Ib. 3-(3-Thienyl)quinuclidin-3-ol Fumarate (17). A solution of *n*-butyllithium in hexane (1.45 M; 14.9 mL, 21.6 mmol) was added over 5 min to a stirred solution of 3-bromothiophene (4.01 g, 24.6 mmol) in ether (40 mL) at −75 °C. After 10 min, a solution of quinuclidin-3-one (2.69 g, 21.5 mmol) in ether (30 mL) was added, and the mixture was stirred at −70 °C for 5 h. A solution of saturated ammonium chloride (15 mL) was added dropwise at −45 °C. The mixture was poured into 2.5 M aqueous hydrochloric acid (40 mL) and was washed with ether (3 × 125 mL). The aqueous layer was alkalinized (pH ∼ 13) with 5 M aqueous sodium hydroxide. Extraction with ether (10 × 150 mL), drying (K_2CO_3) of the

combined organic layers, filtration, and concentration in vacuo gave the crude product. Column chromatography on alumina using $CHCl_3/MeOH$ (95:5) as eluent yielded 2.26 g (50%) of the pure base, which was converted into its fumarate salt and recrystallized. **17**: TLC R_f (free base on alumina) = 0.18 [$CHCl_3/MeOH$ (95:5)]; ^{1}H NMR (89.55 MHz, D_2O) δ 7.43–7.31 (m, thiophene 2-CH and 5-CH), 7.09 (dd, J = 2.1 and 4.7 Hz, thiophene 4-CH), 6.35 (s, 1 H, fumarate CH=CH), 3.88–3.03 (m, 2-CH_2, 6-CH_2, and 7-CH_2), 2.52–1.29 (m, 4-CH, 5-CH_2, and 8-CH_2); ^{13}C NMR (22.5 MHz, D_2O) δ 175.94 (C=O), 145.27 (thiophene C3), 136.78 (fumarate CH=CH), 129.00, 127.17, 123.56, 71.27 (C3), 60.50 (C2), 47.77 and 47.12 (C6 and C7), 32.58 (C4), 20.87 and 19.30 (C5 and C8). Anal. ($C_{11}H_{15}$-NOS·0.5$C_4H_4O_4$) C, H, N.

General Method IIa. 3-(3-Thienyl)quinuclidin-2-ene Fumarate (30). The free base of **17** (800 mg, 3.82 mmol) was dissolved in concentrated formic acid (10 mL). The solution was stirred under reflux for 2.5 h. The solution was made basic with 5 M aqueous sodium hydroxide and extracted with ether (5 × 150 mL). The combined organic layers were dried (K_2CO_3), filtered, and concentrated in vacuo to yield 700 mg (96%) of the pure base. The product was converted into its fumarate salt and recrystallized. **30**: TLC R_f (free base on alumina) = 0.62 [$CHCl_3/MeOH$ (95:5)]; ^{1}H NMR (89.55 MHz, CD_3OD) δ 7.72 (dd, J = 1.3 and 3.2 Hz, thiophene 2-CH), 7.71 (dd, J = 2.7 and 5.1 Hz, thiophene 5-CH), 7.35 (dd, J = 1.3 and 5.0 Hz, thiophene 4-CH), 6.98 (d, J = 1.4 Hz, 2-CH), 6.70 (s, 1 H, fumarate CH=CH), 3.68–2.90 (m, 4-CH, 6-CH_2, and 7-CH_2), 2.27–1.53 (m, 5-CH_2 and 8-CH_2); ^{13}C NMR (22.5 MHz, CD_3OD) δ 174.06 (C=O), 144.07 (thiophene C3), 136.94 (fumarate CH=CH), 136.20 (C3), 128.41, 125.51, 125.05, 124.59, 51.24 (C6 and C7), 30.27 (C4), 25.02 (C5 and C8). Anal. ($C_{11}H_{13}NS$·0.5$C_4H_4O_4$) C, H, N.

3-(3-Benzofuranyl)quinuclidin-2-ene Oxalate (36). A solution of 2,3-dihydrobenzofuran-3-one (4.45 g, 33 mmol) in THF (30 mL) was added to a stirred solution of 3-lithioquinuclidin-2-ene (**34**) [generated from quinuclidin-3-one ((2,4,6-triisopropylphenyl)sulfonyl)hydrazone (**33**; 6.0 g, 14.8 mmol) in THF (150 mL)][17] at 0 °C. The reaction was quenched after 1 h with water (3 mL). The crude mixture was concentrated in vacuo, and the residue was dissolved in concentrated formic acid (20 mL). The mixture was stirred for 1 h at 100 °C, made basic with 5 M aqueous sodium hydroxide, and extracted with $CHCl_3$ (3 × 100 mL). The combined organic layers were dried (K_2CO_3), filtered, and concentrated in vacuo. The residue was purified by repetitive column chromatography, first on alumina using $CHCl_3$ as eluent and then on silica using $CHCl_3$/methanol (90:10) as eluent, to yield 800 mg (24%) of pure base. The product was converted into its oxalate salt and recrystallized. **36**: TLC R_f (free base on silica) = 0.35 ($CHCl_3$/methanol (90:10)); ^{1}H NMR (270 MHz, DMSO-d_6) δ 8.56 (s, benzofuran 2-CH), 7.90–7.84 (m, 1 ArH), 7.69 (m, 1 ArH), 7.47–7.36 (m, 2 ArH's), 7.28 (br s, 2-CH), 3.63–3.47 and 3.17–3.02 (each m, 6-CH_2, 7-CH_2, and 4-CH), 2.11–1.98 and 1.85–1.69 (each m, 5-CH_2 and 8-CH_2); ^{13}C NMR (67.9 MHz, DMSO-d_6) δ 163.34 (C=O), 155.27 (benzofuran C7a), 145.75, 138.27, 125.37, 123.86, 123.72, 123.66, 121.08, 115.00, 111.88, 49.65 (C6 and C7), 28.19 (C4), 23.11 (C5 and C8). Anal. ($C_{15}H_{15}NO$·(COOH)$_2$·1/3H_2O) C, H, N.

General Method IIb. 3-(2-Benzothiazolyl)quinuclidin-2-ene Hydrochloride (39). A stirred mixture **21** (0.55 g of the free base, 2.11 mmol) and methanesulfonic acid (20 mL) was heated at 200 °C for 4 h. Crushed ice (∼100 g) followed by 5 M aqueous sodium hydroxide (until pH 10 was reached) was carefully added to the reaction mixture. Extraction with ether (4 × 150 mL), drying (K_2CO_3) of the combined organic layers, filtration, and concentration in vacuo gave the crude product as a pale yellow solid. This material was purified by column chromatography on alumina using ether as eluent to yield 0.34 g (66%) of the base as a white solid which was converted into its hydrochloride salt and recrystallized. **39**: TLC R_f (free base on alumina) = 0.42 (ether); ^{1}H NMR (89.55 MHz, CD_3OD) δ 8.11–7.98 (m, 2 ArH's), 7.68–7.39 (m, 2-CH and 2 ArH's), 4.14–3.60 and 3.52–3.13 (each m, 3 H and 2 H, respectively, 4-CH, 6-CH_2, and 7-CH_2), 2.44–1.69 (m, 5-CH_2 and 8-CH_2); ^{13}C NMR (22.5 MHz, CD_3OD) δ 161.71 (benzothiazole C2), 154.51 (benzothiazole C3a), 143.42 (C3), 136.13

(benzothiazole C7a), 130.24, 128.11, 127.86, 124.62, 123.19, 51.85 (C6 and C7), 29.49 (C4), 24.18 (C5 and C8). Anal. (C$_{14}$H$_{14}$N$_2$S·HCl) C, H, N.

General Method III. 3-(2-Benzofuranyl)quinuclidine Fumarate (47). The free base of 3-(2-benzofuranyl)quinuclidin-2-ene (**31**; 770 mg, 3.42 mmol) was dissolved in THF (50 mL) and hydrogenated over 10% Pd/C (~0.5 g) at atmospheric pressure during 7.5 h. Filtration through Celite and concentration in vacuo afforded the crude product. This material was chromatographed on an alumina column using ether/methanol (95:5) as eluent. The pure base (0.68 g, 87%) was obtained as a solid which was converted into its fumarate salt and recrystallized. **47**: TLC R_f (free base on alumina) = 0.35 [ether/methanol (95:5)]; ^{1}H NMR (270 MHz, CD$_3$OD) δ 7.58–7.54, 7.47–7.43 and 7.30–7.18 (each m, 1 H, 1 H and 2 H, respectively, ArH's), 6.81 (m, benzofuran 3-CH), 6.69 (s, 2 H, fumarate CH=CH), 3.81–3.60 (m, 2-CH$_2$ and 3-CH), 3.50–3.26 (m, obscured in part by solvent peaks, 6-CH$_2$ and 7-CH$_2$), 2.53–2.48 (m, 4-CH), 2.20–1.81 (m, 5-CH$_2$ and 8-CH$_2$); ^{13}C NMR (22.5 MHz, CD$_3$OD) δ 171.47 (C=O), 158.06 and 156.33 (benzofuran C2 and C7a), 136.20 (fumarate CH=CH), 129.53 (benzofuran C3a), 125.26, 124.03, 121.93, 111.80, 104.45, 50.28 (C2), 47.47 (two coinciding peaks, C6 and C7),[62] 34.90 (C3), 26.19, 24.24, and 19.89 (C4, C5, and C8). Anal. (C$_{15}$H$_{17}$NO·C$_4$H$_4$O$_4$) C, H, N.

3-(2-Tetrahydrofuranyl)quinuclidine Fumarate (45a and 45b). The free base of 3-(2-furanyl)quinuclidin-2-ene (**26**; 1.04 g, 5.94 mmol) was dissolved in THF (55 mL) and hydrogenated over rhodium (5%) on alumina (~0.5 g) at atmospheric pressure during 27 h. The crude reaction mixture, which consisted of a 1:1 mixture of diastereomers together with minor impurities (~9%; GLC), was concentrated in vacuo. The diastereomers (**45a** and **45b**) were separated by repetitive column chromatography on alumina (column size: 23 × 4 cm) using ammonia-saturated CHCl$_3$/n-hexane (7:3)[63] as eluent. The separated diastereomers [≥99% de; GLC (temperature: 130 °C (oven)/300 °C (injector), carrier: 50 kPa) with retention times of 11.9 (**45a**) and 12.5 min (**45b**)] were further purified by two recrystallizations of the fumarate salts. This afforded 270 mg (31%) of **45a** and **45b**, respectively. **45a**: TLC R_f (free base on alumina) = 0.58 [ammonia-saturated CHCl$_3$/n-hexane (3:1)]; ^{1}H NMR (89.55 MHz, CD$_3$-OD) δ 6.67 (s, 2 H, fumarate CH=CH), 4.0–3.5 (m, 4 H), 3.50–3.10 (m, 5 H), 3.02–2.70 (m, 1 H), 2.38–1.70 (m, 8 H), 1.70–1.32 (m, 1 H); ^{13}C NMR (22.5 MHz, CD$_3$OD) δ 171.41 (C=O), 136.20 (fumarate CH=CH), 79.65 (tetrahydrofuran C2), 68.93 (tetrahydrofuran C5), 49.85, 47.62, and 47.22 (C2, C6, and C7), 40.12 (C3), 30.39, 26.47, 24.89, 22.64, and 19.27 (C4, C5, C8, and tetrahydrofuran β C's). Anal. (C$_{11}$H$_{19}$NO·C$_4$H$_4$O$_4$) C, H, N.

45b: TLC R_f (free base on alumina) = 0.36 [ammonia-saturated CHCl$_3$/n-hexane (3:1)]; ^{1}H NMR (89.55 MHz, CD$_3$-OD) δ 6.67 (s, 2 H, fumarate CH=CH), 4.02–3.50 (m, 4 H), 3.50–3.06 (m, 6 H), 2.30–1.36 (m, 9 H); ^{13}C NMR (22.5 MHz, CD$_3$OD) δ 171.40 (C=O), 136.20 (fumarate CH=CH), 81.75 (tetrahydrofuran C2), 68.99 (tetrahydrofuran C5), 50.96 (C2), 47.65 and 47.10 (C6 and C7), 39.87 (C3), 31.25, 26.46, 25.48, 24.46, and 19.98 (C4, C5, C8, and tetrahydrofuran β C's). Anal. (C$_{11}$H$_{19}$NO·C$_4$H$_4$O$_4$) C, H, N.

***N*-(Chloromethyl)-3-(2-tetrahydrofuranyl)quinuclidinium Chloride (46).** The fumarate salt of **45b** (134 mg, 0.45 mmol) was converted into the free base by alkalization (aqueous K$_2$CO$_3$), extraction with CHCl$_3$, drying (K$_2$CO$_3$) of the organic layer, filtration, and concentration in vacuo. The resulting oil was dissolved in CH$_2$Cl$_2$ (9 mL) and stirred for 20 h at room temperature. Concentration in vacuo gave an oily residue which was triturated with ether to remove traces of starting material. This afforded pure (TLC) but hygroscopic **46** as a white powder. Drying under vacuum gave 110 mg (92%) of **46**: ^{1}H NMR (270 MHz, CDCl$_3$) δ 5.88 (narrow m, CH$_2$-Cl), 4.20–3.50 (m, 9 H), 2.44 (s, 1 H), 2.40–1.80 (m, 8 H), 1.57–1.35 (m, 1 H); ^{13}C NMR (67.9 MHz, CDCl$_3$) δ 79.80 (tetrahydrofuran C2), 77.41 (CH$_2$Cl), 68.39 (tetrahydrofuran C5), 55.90, 53.67, and 53.40 (C2, C6, and C7), 39.14 (C3), 30.46, 25.39, 25.28, 24.24, and 20.14 (C4, C5, C8, and tetrahydrofuran β C's). Anal. (C$_{12}$H$_{21}$Cl$_2$NO) C, H, N.

3-(2,3-Dihydrobenzofuran-2-yl)quinuclidine Fumarate

(48a and 48b). The free base of **47** (6.87 g, 30.4 mmol) was dissolved in glacial acetic acid (200 mL) and hydrogenated over 10% Pd/C (~1 g) at atmospheric pressure during 50 h. The reaction mixture was filtered through Celite, alkalinized with aqueous 5 M sodium hydroxide, and extracted with ether (5 × 200 mL). The combined organic layers were dried (K$_2$CO$_3$), filtered, and concentrated in vacuo. This afforded the crude product (5.7 g, 81%) as a solid which consisted of a 1:1 mixture of diastereomers **48a** and **48b** [GLC analysis; temperature, 160 °C (oven)/280 °C (injector); carrier, 80 kPa) with retention times of 17.9 (**48a**) and 18.7 min (**48b**)]. A portion of the diastereomeric mixture (2.01 g) was separated by repetitive flash chromatography on silica gel (column size: 23 × 4 cm) using a gradient of ammonia-saturated ether/methanol (95:5 → 93:7) as eluent. This afforded 750 mg (75%) of **48a** [≥99% de (by GLC)] and 590 mg (59%) of **48b** [≥99% de (by GLC)]. The bases were converted into their fumarate salts and recrystallized. **48a**: TLC R_f (free base on silica) = 0.33 [ammonia-saturated ether/methanol (92:8)]; ^{1}H NMR (270 MHz, DMSO-d_6) δ 7.20, 7.07, 6.81 (each m, each 1 ArH), 6.73 (app d, J = 7.9 Hz, 1 ArH), 6.42 (s, 1 H, fumarate CH=CH), 4.80 (ddd, J = 8.8, 9.2 and 9.2 Hz, dihydrobenzofuran 2-CH), 3.30 (dd, J = 8.7 and 15.7 Hz, dihydrobenzofuran 3-CH), 3.18 (dd, J = 11.5 and 13.8 Hz, 2-CH), 3.03–2.84 (m, 6-CH$_2$ and 7-CH$_2$), 2.80 (dd, J = 7.7 and 15.7 Hz, dihydrobenzofuran 3-CH), 2.56 (ddd, J = 1.5, 6.6, and 13.0 Hz, 2-CH), 2.14–1.98, 1.98–1.80, and 1.78–1.46 (each m, 2 H, 1 H and 3 H, respectively, 3-CH, 4-CH, 5-CH$_2$, and 8-CH$_2$); ^{13}C NMR (22.5 MHz, CD$_3$OD) δ 172.92 (C=O), 160.26 (dihydrobenzofuran C7a), 136.60 (fumarate CH=CH), 129.09, 127.27 (dihydrobenzofuran C3a), 126.16, 121.81, 110.16, 82.86 (dihydrobenzofuran C2), 49.23, 47.50, and 47.13 (C2, C6, and C7), 40.03 (C3), 34.31 (dihydrobenzofuran C3), 24.80, 22.33, and 19.33 (C4, C5, and C8). Anal. (C$_{15}$H$_{19}$NO·0.5C$_4$H$_4$O$_4$) C, H, N.

48b: TLC R_f (free base on silica) = 0.40 [ammonia-saturated ether/methanol (92:8)]; ^{1}H NMR (270 MHz, DMSO-d_6) δ 7.20, 7.08, 6.82 (each m, each 1 ArH), 6.76 (app d, J = 7.9 Hz, 1 ArH), 6.46 (s, 2 H, fumarate CH=CH), 4.89 (ddd, J's = 9.0 Hz, dihydrobenzofuran 2-CH),[64] 3.32 (m, 2-CH),[65] 3.27 (dd, J = 9.0 and 15.7 Hz, dihydrobenzofuran 3-CH),[65] 3.14–2.98 (m, 2-CH, 6-CH$_2$, and 7-CH$_2$), 2.91 (dd, J = 7.9 and 15.7 Hz, dihydrobenzofuran 3-CH), 2.14 (m, 3-CH), 1.98–1.84, 1.82–1.70, and 1.70–1.56 (each m, 2 H, 2 H, and 1 H, respectively, 4-CH, 5-CH$_2$, and 8-CH$_2$); ^{13}C NMR (22.5 MHz, CD$_3$OD) δ 171.47 (C=O), 160.35 (dihydrobenzofuran C7a), 136.20 (fumarate CH=CH), 129.09, 127.55 (dihydrobenzofuran C3a), 126.10, 121.81, 110.26, 85.27 (dihydrobenzofuran C2), 50.80, 47.65, and 47.10 (C2, C6, and C7), 40.24 (C3), 35.11 (dihydrobenzofuran C3), 25.32, 23.53, and 19.80 (C4, C5, and C8). Anal. (C$_{15}$H$_{19}$NO·C$_4$H$_4$O$_4$) C, H, N.

General Method IV. 3-(2-Benzofuranyl)quinuclidin-3-ol Methiodide (49). An excess of iodomethane (3.40 g, 24 mmol) was added to a stirred solution of 3-(2-benzofuranyl)quinuclidin-3-ol (**18**; 584 mg of the free base, 2.4 mmol) in acetone at room temperature. This solution was stirred for 6 h. The resulting quaternary ammonium salt was collected by filtration and triturated with acetone. This gave 798 mg (86%) of **49**: ^{1}H NMR (270 MHz, CD$_3$OD) δ 7.62, 7.51 and 7.35–7.22 (each m, 1 H, 1 H and 2 H, respectively, ArH's), 7.03 (d, $J_{3-H,7-H}$ = 0.9 Hz, benzofuran 3-CH), 4.22 (dd, J = 2.5 and 13.3 Hz, 2-CH), 3.70–3.40 (m, 2-CH, 6-CH$_2$, and 7-CH$_2$), 3.16 (s, CH$_3$), 2.73–2.68, 2.62–2.52, and 2.15–1.83 (each m, 1 H, 1 H, and 3 H, respectively, 4-CH, 5-CH$_2$, and 8-CH$_2$); ^{13}C NMR (67.9 MHz, DMSO-d_6) δ 158.00 and 154.08 (benzofuran C2 and C7a), 127.36, 124.65, 123.03, 121.31, 111.10, 103.66, 68.46 and 66.34 (C2 and C3), 55.59 and 54.77 (C6 and C7), 50.87 (CH$_3$), 29.48 (C4), 20.69 and 18.83 (C5 and C8). Anal. (C$_{16}$H$_{20}$INO$_2$) C, H, N.

Determination of Ionization Constants.[66] pK_a's were determined by potentiometric titration using a calibrated (buffers pH 7 and 10, Titrisol, Merck) glass pH electrode with an internal reference electrode (Mettler DG 111-SC) and an automatic titrator (Mettler DL25). The hydrochloride salt was dissolved in 50 mL of 0.1 M potassium chloride in carbonate-free water, giving a concentration of 0.005–0.01 M. The titration was performed with 0.1 M sodium hydroxide (Titrisol, Merck) by constant volume addition of 0.05 mL at 25 ± 1 °C.

Quinuclidine hydrochloride was used as a reference substance; observed $pK_a = 11.29$ (lit.[27a] $pK_a = 11.29$). Obtained pK_a values are mean values of two or more independent measurements.

Molecular Modeling. The semiempirical methods AM1 and PM3 were used as implemented in the MOPAC package (version 5.0). The convergence criterion PRECISE was used. The structures were built, manipulated, and displayed in SYBYL 6.0[67] on an Evans and Sutherland ESV workstation (Evans and Sutherland Computer Corporation). Molecular mechanics calculations were performed using the MMX-89.0 force field as included in the PCMODEL program. The dihedral facility in MMX was used. For alcohol **13** the H-BND option was activated during the dihedral driver process in order to take into account intramolecular hydrogen bonding. All calculations of electrostatic potentials were performed in SPARTAN 3.0.[68] Electron density surfaces were displayed at 0.002 e/au³.

Pharmacology. Muscarinic Receptor Binding Studies. The tissue preparations and the general methods used have been described in detail elsewhere for the parotid gland,[38] urinary bladder,[39] heart,[40] and cerebral cortex,[40] respectively. Male guinea pigs (250–400 g of body weight) were killed by a blow on the neck and exsanguinated. The brain was placed on ice for dissection of the cerebral cortex (gray matter only). Urinary bladders, hearts, and parotid glands were dissected in a Krebs–Henseleit buffer (pH 7.4) containing 1 mM α-toluenesulfonyl fluoride (PMSF; Sigma), a protease inhibitor. The Krebs–Henseleit buffer was composed of the following (mM): NaCl 118.0, KCl 5.36, CaCl₂ 2.52, MgSO₄ 0.57, and NaH₂PO₄ 1.17, NaHCO₃ 25.0, and glucose 11.1. Dissected tissues were homogenized in an ice-cold sodium–potassium phosphate buffer (50 mM, pH 7.4) containing 1 mM PMSF, using a Polytron PT-10 instrument (bladder, heart, parotid) and a Potter–Elvehjem Teflon glass homogenizer (cortex). All homogenates were diluted with ice-cold phosphate/PMSF buffer to a final protein concentration of ≤0.3 mg/mL and were immediately used in the receptor-binding assays. Protein was determined by the method of Lowry et al.,[69] using bovine serum albumin as the standard.

The muscarinic receptor affinities of the unlabeled compounds were derived from competition experiments in which the ability to inhibit the receptor specific binding of (−)-[³H]-QNB (3-quinuclidinyl [*phenyl*-4-³H]benzilate, 32.9–45.4 Ci/mmol) was monitored as previously described.[40,41] Each sample contained 10 μL of (−)-[³H]QNB solution (final concentration 2 nM), 10 μL of a solution of test compound, and 1.0 mL of tissue homogenate. Triplicate samples were mixed and incubated under conditions of equilibrium, i.e., at 25 °C for 60 (urinary bladder), 80 (heart and cerebral cortex), or 210 (parotid gland) min. Nonspecific binding was determined in the presence of 10 μM unlabeled atropine. Incubations were terminated by centrifugation,[39] and the radioactivity in the pellets was determined by liquid scintillation spectrometry.[39] IC_{50} values (concentration of unlabeled compound producing 50% inhibition of the receptor specific (−)-[³H]QNB binding) were graphically determined from the experimental concentration–inhibition curves. Affinities, expressed as the inhibition constants, K_i, were calculated by correcting the IC_{50} for the radioligand-induced parallel shift and differences in receptor concentration, using the method of Jacobs et al.[70] The binding parameters for (−)-[³H]QNB (K_D and receptor densities) used in these calculations have been determined in a separate series of experiments.[38–40]

Functional in Vitro Studies. Male guinea pigs, weighing about 300 g, were killed by a blow on the neck and exsanguinated. Smooth muscle strips of the urinary bladder were dissected in a Krebs–Henseleit solution (pH 7.4). The strip preparations were vertically mounted between two hooks in thermostatically controlled (37 °C) organ baths (5 mL). One of the hooks was adjustable and connected to a force transducer (FT 03, Grass Instruments). The Krebs–Henseleit solution was continuously bubbled with carbogen gas (93.5% O₂/6.5% CO₂) to maintain the pH at 7.4. Isometric tension was recorded by a Grass Polygraph (Model 79D). A resting tension of approximately 5 mN was initially applied on each muscle strip, and the preparations were allowed to stabilize for at least 45 min. The resting tension was adjusted, and the preparations were washed several times during the stabilization. The urinary bladder strips were used for evaluation of antimuscarinic activity (see Pharmacological Results). Carbachol (carbamylcholine chloride) was used as the agonist. Concentration–response curves to carbachol were generated by cumulative dose–response technique.

A control concentration–response curve to carbachol was generated by cumulative addition of carbachol to the bladder strip (i.e., stepwise increase of the agonist concentration until the maximal contractile response was reached), followed by washing out and a resting period of at least 15 min prior to addition of a fixed concentration of the test compound to the organ bath. After 60 min of incubation, a second cumulative concentration–response curve to carbachol was generated. Responses were expressed as percent of the maximal response to carbachol. EC_{50} values for carbachol in the absence (control) and presence of antagonist were graphically derived and dose ratios (r) were calculated. Concentrations of test compound producing at least a 4-fold increase of the EC_{50} value for carbachol were used when calculating the dissociation constant, K_B, for the antagonists; $K_B = [A]/(r - 1)$, where [A] is the concentration of the test compound.[71]

Supplementary Material Available: ¹H NMR and ¹³C NMR spectral data for **13–16, 18–20, 22–24, 26–29, 31, 32, 37, 38, 40–43,** and **50–52a,b** and ¹³C NMR spectral data for **25, 44,** and **47** (10 pages). Ordering information is given on any masthead page.

References

(1) (a) Saunders, J.; Cassidy, M.; Freedman, S. B.; Harley, E. A.; Iversen, L. L.; Kneen, C.; MacLeod, A. M.; Merchant, K. J.; Snow, R. J.; Baker, R. Novel Quinuclidine-Based Ligands for the Muscarinic Cholinergic Receptor. *J. Med. Chem.* **1990**, *33*, 1128–1138. (b) Street, L. J.; Baker, R.; Book, T.; Kneen, C. O.; MacLeod, A. M.; Merchant, K. J.; Showell, G. A.; Saunders, J.; Herbert, R. H.; Freedman, S. B.; Harley, E. A. Synthesis and Biological Activity of 1,2,4-Oxadiazole Derivatives. Highly Potent and Efficacious Agonists for Cortical Muscarinic Receptors. *J. Med. Chem.* **1990**, *33*, 2690–2697. (c) Orlek, B. S.; Blaney, F. E.; Brown, F.; Clark, M. S. G.; Hadley, M. S.; Hatcher, J.; Riley, G. J.; Rosenberg, H. E.; Wadsworth, H. J.; Wyman, P. Comparison of Azabicyclic Esters and Oxadiazoles as Ligands for the Muscarinic Receptor. *J. Med. Chem.* **1991**, *34*, 2726–2735. (d) Showell, G. A.; Gibbons, T. L.; Kneen, C. O.; MacLeod, A. M.; Merchant, K.; Saunders, J.; Freedman, S. B.; Patel, S.; Baker, R. Tetrahydropyridyloxadiazoles: Semirigid Muscarinic Ligands. *J. Med. Chem.* **1991**, *34*, 1086–1094.

(2) Compare also: Triggle, D. J.; Kwon, Y. W.; Abraham, P.; Rahman, M. A.; Carroll, F. I. Synthesis of 2-(3-Substituted-1,2,4-oxadiazol-5-yl)-8-methyl-8-azabicyclo[3,2,1]octanes and 2α-(3-Substituted-1,2,4-oxadiazol-5-yl)-8-methyl-8-azabicyclo[3,2,1]oct-2-enes as Potential Muscarinic Agonists. *Pharm. Res.* **1992**, *9*, 1474–1479.

(3) MacLeod, A. M.; Baker, R.; Freedman, S. B.; Patel, S.; Merchant, K. J.; Roe, M.; Saunders, J. Synthesis and Muscarinic Activities of 1,2,4-Thiadiazoles. *J. Med. Chem.* **1990**, *33*, 2052–2059.

(4) Jenkins, S. M.; Wadsworth, H. J.; Bromidge, S.; Orlek, B. S.; Wyman, P. A.; Riley, G. J.; Hawkins, J. Substituent Variation in Azabicyclic Triazole- and Tetrazole-Based Muscarinic Receptor Ligands. *J. Med. Chem.* **1992**, *35*, 2392–2406.

(5) Street, L. J.; Baker, R.; Book, T.; Reeve, A. J.; Saunders, J.; Willson, T.; Marwood, R. S.; Patel, S.; Freedman, S. B. Synthesis and Muscarinic Activity of Quinuclidinyl- and (1-Azanorbornyl)-pyrazine Derivatives. *J. Med. Chem.* **1992**, *35*, 295–305.

(6) Lambrecht, G.; Mutschler, E. Struktur- und Konformations-Wirkungs-Beziehungen bei Zyklischen Acetylcholinanaloga der Piperidin- und Chinuclidin-Reihe. (Structure- and conformation-activity relationships of cyclic acetylcholine analogs of the quinuclidine and piperidine series.) *Arzneim. Forsch.* **1974**, *24*, 1725–1729.

(7) Compound **3**, the 2,3-dehydro analogue of **1**, had similar affinity and efficacy at ileal muscarinic receptors as **1**. On the other hand, the 2,3-dehydro analogue of the antagonist **2** (i.e., **4**) had about 4-fold lower affinity for ileal muscarinic receptors than **2**.[6]

(8) Affinities to rat cerebral cortex, using the agonist [³H]oxotremorine-M (OXO-M) as the radioligand, of quinuclidin-2-ene derivatives substituted in the 3-position with a 1,2,5-thiadiazole moiety were lower than those for the corresponding quinuclidine congeners. See: Sauerberg, P.; Olesen, P. H. International Patent No. WO 92/03433, 1992; *Chem. Abstr.* **1993**, *118*, 234062d.

(9) Other quinuclidine-based muscarinic antagonists have been reported. See, e.g.: (a) Baumgold, J.; Cohen, V. I.; Paek, R.; Reba, R. C. Muscarinic Receptor Subtype Selectivity of Novel Heterocyclic QNB Analogues. *Life Sci.* **1991**, *48*, 2325–2329. (b) Nilsson, J. L. G.; Wågermark, J.; Dahlbom, R. Potential Antiparkinsonism Agents. *J. Med. Chem.* **1969**, *12*, 1103–1105. (c) Nilsson, J. L. G.; Wågermark, J.; Dahlbom, R. Some Quinuclidine Derivatives with Potential Antimalarial Activity. *Acta Pharm. Suec.* **1968**, *5*, 71–76. (d) Rzeszotarski, W. J.; Gibson, R. E.; Eckelman, W. C.; Simms, D. A.; Jagoda, E. M.; Ferreira, N. L.; Reba, R. C. Analogues of 3-Quinuclidinyl Benzilate. *J. Med. Chem.* **1982**, *25*, 1103–1106.

(10) Orlek, B. S.; Wyman, P. A.; Wadsworth, H. J. Eur. Patent No. 0322 182 A2, 1989; *Chem. Abstr.* **1990**, *112*, 138925t.

(11) (a) Reed, F. D.; Burger, A. Quinuclidine Analogs of Tobacco Alkaloids. *J. Med. Chem.* **1971**, *14*, 554–556. (b) Baker, R.; Saunders, J.; Willson, T.; Kulagowski, J. J. Eur. Patent No. 0412 798 A2, 1991; *Chem. Abstr.* **1991**, *115*, 8590f.

(12) Baker, R.; Showell, G. A. Eur. Patent No. 0412 797 A2, 1991; *Chem. Abstr.* **1991**, *115*, 8596n.

(13) For a review, see: Gschwend, H. W.; Rodriguez, H. R. Heteroatom-Facilitated Lithiations. *Org. React.* **1979**, *26*, 1–360.

(14) For numerous examples of halogen-metal exchange, see: (a) Wakefield, B. J. *The Chemistry of Organolithium Compounds*; Pergamon Press: Oxford, 1974. (b) Wakefield, B. J. *Organolithium Methods*; Academic Press: London, 1988; Chapter 3.

(15) See: (a) Gilman, H.; Melstrom, D. S. 2-Benzofuryllithium and 3-Benzofuryllithium. *J. Am. Chem. Soc.* **1948**, *70*, 1655–1657. (b) Cugnon de Sévricourt, M.; Robba, M. *Bull. Soc. Chim. Fr.* **1977**, 142–144. (c) Barton, T. J.; Groh, B. L. Gas-Phase Thermal Rearrangement of Potential Vinylidene Precursors to Silylbenzofurans and Silylbenzopyrans. *J. Org. Chem.* **1985**, *50*, 158–166.

(16) See, e.g.: (a) ref 14b, pp 49–50. (b) Adlington, R. M.; Barrett, A. G. M. Recent Applications of the Shapiro Reaction. *Acc. Chem. Res.* **1983**, *16*, 55–59.

(17) Nordvall, G.; Hacksell. U. *Bioorg. Med. Chem. Lett.* In press.

(18) A similar observation was made in an attempt to demethylate 3-(4-methoxyphenyl)quinuclidin-2-ene: Grob, C. A.; Kaiser, A.; Renk, E. 2-Dehydro-chinuclidin und Einige 3-Substitutionsprodukte. Untersuchungen in der Chinuclidinreihe. 5. Mitteilung. (2-Dehydroquinuclidine and some 3-substituted derivatives. Studies of the quinuclidines. Part 5.) *Helv. Chim. Acta* **1957**, *40*, 2170–2185.

(19) For the generation of lithium o-lithiophenoxide, see: Talley, J. J.; Evans, I. A. Reactions of Lithium o-Lithiophenoxide with Carbonyl Compounds. *J. Org. Chem.* **1984**, *49*, 5267–5269.

(20) The synthesis and muscarinic properties of **44** have been described in ref 1a. For an alternative synthetic procedure, see ref 10.

(21) The choice of catalyst may influence the course of reduction of furan derivatives: (a) Rylander, P. N. *Hydrogenation Methods*; Academic Press: London, 1985; pp 133–134 and references cited therein. (b) Pachaly, P. In *Methoden der Organischen Chemie (Houben-Weyl)*, 4th ed.; Georg Thieme Verlag: Stutttgart, 1980; Vol. IV/1c, "Reduktion Teil I", pp 331–346 and references cited therein.

(22) The relative stereochemistry of the diastereomers was not established.

(23) Hydrogenation of benzofuran to 2,3-dihydrobenzofuran has been accomplished under similar conditions: Ellison, R. A.; Kotsonis, F. N. Complexation as a Factor in Metalation Reactions. Metalation of 1-Methoxy-2-phenoxyethane. *J. Org. Chem.* **1973**, *38*, 4192–4196.

(24) For an application of ionic hydrogenation to benzofuran, see: (a) Karakhanov, E. A.; Dem'yanova, E. A.; Shkarin, E. G.; Viktorova, E. A. *Khim. Geterotsikl. Soedin.* **1975**, *11*, 1479–1481; *Chem. Abstr.* **1976**, *84*, 89923h. (b) For a review, see: Kursanov, D. N.; Parnes, Z. N.; Loim, N. M. Applications of Ionic Hydrogenation to Organic Synthesis. *Synthesis* **1974**, 633–651.

(25) (a) Becker, K. B.; Grob, C. A. ¹³C-NMR. Spectra of 4-Substituted Quinuclidines. Polar Effects, Part V. *Helv. Chim. Acta* **1978**, *61*, 2596–2606. (b) Valckx, L. A.; Borremans, F. A. M.; Becu, C. E.; De Waele, R. H. K.; Anteunis, M. J. O. The Stereochemical Dependence of the Vicinal ¹³C-¹⁴N Coupling Constant as a Constitutional Probe. *Org. Magn. Reson.* **1979**, *12*, 302–305.

(26) However, it has been claimed that the nonprotonated form may also contribute to the affinity for the muscarinic receptor. See, e.g.: (a) Burgen, A. S. V. The Role of Ionic Interaction at the Muscarinic Receptor. *Br. J. Pharmacol.* **1965**, *25*, 4–17. (b) Ehlert, F. J.; Delen, F. M. Influence of pH on the Binding of Scopolamine and N-Methylscopolamine to Muscarinic Receptors in the Corpus Striatum and Heart of Rats. *Mol. Pharmacol.* **1990**, *38*, 143–147 and references cited therein.

(27) The pK_a values of (a) quinuclidin-3-ol (9.91), (b) quinuclidin-2-ene (9.88), and (c) 3-phenylquinuclidin-2-ene (9.10) have been reported: (a) Grob, C. A. Inductive Charge Dispersal in Quinuclidinium Ions. *Helv. Chim. Acta* **1985**, *68*, 882–886. (b) Grob, C. A. Polare Effekte bei Organischen Reaktionen. *Angew. Chem.* **1976**, *88*, 621–627. (c) Grob, C. A.; Kaiser, A.; Renk, E. Electrostatic Effects in the Ground and Excited States of Mesomeric Molecules. *Chem. Ind.* **1957**, 598–599.

(28) In the calculation of the pK_a value for **39** only data points obtained at pH < 7.5 were used due to start of precipitation at pH 7.5.

(29) Dewar, M. J. S.; Zoebisch, E. G.; Healy, E. F.; Stewart, J. J. P. AM1: A New General Purpose Quantum Mechanical Molecular Model. *J. Am. Chem. Soc.* **1985**, *107*, 3902–3909.

(30) (a) Stewart, J. J. P. Optimization of Parameters for Semiempirical Methods. I. Method. *J. Comput. Chem.* **1989**, *10*, 209–220. (b) Stewart, J. J. P. Optimization of Parameters for Semiempirical Methods. II. Applications. *J. Comput. Chem.* **1989**, *10*, 221–264.

(31) (a) MMX is a molecular mechanics program that is an enhanced version of Allinger's MMP2-program. The MMX program is part of the molecular modeling package PCMODEL (Serena Software, P.O. Box 3076, Bloomington, IN 47402-3076). (b) Gajewski, J. J.; Gilbert, K. E.; McKelvey, J. MMX an Enhanced Version of MM2. *Adv. Mol. Modeling* **1990**, *2*, 65–92.

(32) Only PM3 calculations were carried out.

(33) Ab initio molecular orbital calculations performed on the 2- and 3-vinyl derivatives of furan and thiophene, respectively, indicate the same preference for coplanar conformations: (a) John, I. G.; Radom, L. Conformations, Stabilities, and Charge Distributions in 2- and 3-Monosubstituted Furans. An ab Initio Molecular Orbital Study. *J. Am. Chem. Soc.* **1978**, *100*, 3981–3991. (b) Kao, J.; Radom, L. Conformations, Stabilities, and Charge Distributions in 2- and 3-Monosubstituted Thiophenes. An ab Initio Molecular Orbital Study. *J. Am. Chem. Soc.* **1979**, *101*, 311–318.

(34) It may be noted that the AM1 and PM3 methods have a tendency to underestimate rotational barriers around single bonds in conjugated molecules compared to ab initio calculations and experimental data. See, e.g.: (a) Fabian, W. M. F. AM1 Calculations of Rotation around Essential Single Bonds and Preferred Conformations in Conjugated Molecules. *J. Comput. Chem.* **1988**, *9*, 369–377. (b) Gundertofte, K.; Palm, J.; Pettersson, I.; Stamvik, A. A. Comparison of Conformational Energies Calculated by Molecular Mechanics (MM2(85), Sybyl 5.1, Sybyl 5.21, and ChemX) and Semiempirical (AM1 and PM3) Methods. *J. Comput. Chem.* **1991**, *12*, 200–208.

(35) For UV spectral properties of furan and benzofuran derivatives, see: Dean, F. M.; Sargent, M. V. In *Comprehensive Heterocyclic Chemistry*; Katritzky, A. R., Rees, C. W., Eds.; Pergamon Press: Oxford, 1984; Vol. 4, pp 531–597 and references cited therein.

(36) Hariharan, P. C.; Pople, J. A. Effect of d-Functions on Molecular Orbital Energies for Hydrocarbons. *Chem. Phys. Lett.* **1972**, *16*, 217–219.

(37) For subclassification of muscarinic receptors, see: (a) Doods, H. N.; Mathy, M.-J.; Davidesko, D.; van Charldorp, K. J.; de Jonge, A.; van Zwieten, P. A. Selectivity of Muscarinic Antagonists in Radioligand and in Vivo Experiments for the Putative M_1, M_2 and M_3 Receptors. *J. Pharmacol. Exp. Ther.* **1987**, *242*, 257–262. (b) Caulfield, M. P. Muscarinic Receptors: Characterization, Coupling and Function. *Pharmacol. Ther.* **1993**, *58*, 319–379. (c) Watson, S.; Girdlestone, D. Receptor & Ion Channel Nomenclature Supplement, 5th ed. *Trends Pharmacol. Sci.* **1994**, *15* (Suppl.), 30.

(38) Nilvebrant, L.; Sparf, B. Muscarinic Receptor Binding in the Parotid Gland. Different Affinities of Some Anticholinergic Drugs Between the Parotid Gland and Ileum. *Scand. J. Gastroenterol.* **1982**, *17* (Suppl. 72), 69–77.

(39) Nilvebrant, L.; Sparf, B. Muscarinic Receptor Binding in the Guinea Pig Urinary Bladder. *Acta Pharmacol. Toxicol.* **1983**, *52*, 30–38.

(40) Nilvebrant, L.; Sparf, B. Dicyclomine, Benzhexol and Oxybutynin Distinguish Between Sub-Classes of Muscarinic Binding-sites. *Eur. J. Pharmacol.* **1986**, *123*, 133–143.

(41) Nilvebrant, L.; Sparf, B. Differences Between Binding Affinities of Some Antimuscarinic Drugs in the Parotid Gland and those in the Urinary Bladder and Ileum. *Acta Pharmacol. Toxicol.* **1983**, *53*, 304–313.

(42) (a) Hammer, R. B.; Berrie, C. P.; Birdsall, N. J. M.; Burgen, A. S. V.; Hulme, E. C. Pirenzepine Distinguishes Between Different Subclasses of Muscarinic Receptors. *Nature* **1980**, *283*, 90–92. (b) Hammer, R.; Giachetti, A. Muscarinic Receptor Subtypes: M1 and M2 Biochemical and Functional Characterization. *Life Sci.* **1982**, *31*, 2991–2998.

(43) (a) Giachetti, A.; Micheletti, R.; Montagna, E. Cardioselective Profile of AF-DX 116, a Muscarine M_2 Antagonist. *Life Sci.* **1986**, *38*, 1663–1672. (b) Hammer, R.; Giraldo, E.; Schiavi, G. B.; Montagna, E.; Ladinsky, H. Binding Profile of a Novel Cardioselective Muscarine Receptor Antagonist, AF-DX 116, to Membranes of Peripheral Tissues and Brain in the Rat. *Life Sci.* **1986**, *38*, 1653–1662.

(44) The data reported for these compounds refer to the racemic mixtures.

(45) The calculations were performed on **13** and **44**.

(46) The replacement of oxygen with sulfur in muscarinic ligands has influenced muscarinic activity differently. For example, the classical muscarinic agonist (5-methylfurfuryl)trimethylammonium iodide has about 100-fold higher muscarinic activity on the guinea pig ileum than the corresponding thiophene analogue. This activity difference was rationalized in terms of relative *O*- and *S*-hydrogen bond strengths and conformational factors: Floersheim, P.; Pombo-Villar, E.; Shapiro, G. Isosterism and Bioisosterism Case Studies with Muscarinic Agonists. *Chimia* **1992**, *46*, 323–334.

(47) Hunter, C. A.; Sanders, J. K. M. The Nature of π-π Interactions. *J. Am. Chem. Soc.* **1990**, *112*, 5525–5534.

(48) For similar suggestions, see: (a) Weinstein, H.; Maayani, S.; Srebrenik, S.; Cohen, S.; Sokolovsky, M. Psychotomimetic Drugs as Anticholinergic Agents. II. Quantum-Mechanical Study of Molecular Interaction Potentials of 1-Cyclohexylpiperidine Derivatives with the Cholinergic Receptor. *Mol. Pharmacol.* **1973**, *9*, 820–834. (b) Melchiorre, C.; Quaglia, W.; Picchio, M. T.; Giardinà, D.; Brasili, L.; Angeli, P. Structure–Activity Relationships among Methoctramine-Related Polymethylene Tetramines. Chain-Length and Substituent Effects on M-2 Muscarinic Receptor Blocking Activity. *J. Med. Chem.* **1989**, *32*, 79–84.

(49) Hydrogen bonds which involve aromatic π electrons have been suggested previously for furan and thiophene. See, e.g.: (a) Yoshida, Z.; Ōsawa, E. Hydrogen Bonding of Phenol to π Electrons of Aromatics, Polyolefins, Heteroaromatics, Fulvenes, and Azulenes. *J. Am. Chem. Soc.* **1966**, *88*, 4019–4026. (b) Bicca De Alencastro, R. A Low Temperature Infrared Study on the Association of Thiols with Organic Oxygen Bases. *Can. J. Chem.* **1974**, *52*, 738–743.

(50) Levitt, M.; Perutz, M. F. Aromatic Rings Act as Hydrogen Bond Acceptors. *J. Mol. Biol.* **1988**, *201*, 751–754.

(51) The hydrogen bond basicities of furan, thiophene, are low and appear to be very similar. See: (a) Abraham, M. H.; Grellier, P. L.; Prior, D. V.; Morris, J. J.; Taylor, P. J. Hydrogen Bonding. Part 10. A Scale of Solute Hydrogen-bond Basicity using log K Values for Complexation in Tetrachloromethane. *J. Chem. Soc., Perkin Trans. 2* **1990**, 521–529. (b) Abraham, M. H. Scales of Solute Hydrogen-bonding: Their Construction and Application to Physicochemical and Biochemical Processes. *Chem. Soc. Rev.* **1993**, 73–83.

(52) Benzofuran and benzothiophene as well as furan and thiophene have similar hydrogen bond basicities.[51b]

(53) Abraham, M. H.; Duce, P. P.; Prior, D. V.; Barratt, D. G.; Morris, J. J.; Taylor, P. J. Hydrogen Bonding. Part 9. Solute Proton Donor and Proton Acceptor Scales for Use in Drug Design. *J. Chem. Soc., Perkin Trans. 2* **1989**, 1355–1375.

(54) Wolf-Pflugmann, M.; Lambrecht, G.; Wess, J.; Mutschler, E. Synthesis and Muscarinic Activity of a Series of Tertiary and Quaternary *N*-Substituted Guvacine Esters Structurally Related to Arecoline and Arecaidine Propargyl Ester. *Arzneim.-Forsch./ Drug Res.* **1989**, *39*, 539–544.

(55) Compare: (a) Weinstein, H.; Maayani, S.; Srebrenik, S.; Cohen, S.; Sokolovsky, M. A Theoretical and Experimental Study of the Semirigid Cholinergic Agonist 3-Acetoxyquinuclidine. *Mol. Pharmacol.* **1975**, *11*, 671–689 and references cited therein. (b) Schulman, J. M.; Sabio, M. L.; Disch, R. L. Recognition of Cholinergic Agonists by the Muscarinic Receptor. 1. Acetylcholine and Other Agonists with the NCCOCC Backbone. *J. Med. Chem.* **1983**, *26*, 817–823.

(56) Nordvall, G.; Hacksell, U. Binding-Site Modeling of the Muscarinic m1 receptor: A Combination of Homology-Based and Indirect Approaches. *J. Med. Chem.* **1993**, *36*, 967–976.

(57) Fraser, C. M.; Wang, C.-D.; Robinson, D. A.; Gocayne, J.; Venter, J. C. Site-Directed Mutagenesis of m1 Muscarinic Acetylcholine Receptors: Conserved Aspartic Acids Play Important Roles in Receptor Function. *Mol. Pharmacol.* **1989**, *36*, 840–847.

(58) Wess, J.; Gdula, D.; Brann, M. R. Structural Basis of the Subtype Selectivity of the Muscarinic Antagonists: A Study with Chimeric m2/m5 Muscarinic Receptors. *Mol. Pharmacol.* **1992**, *41*, 369–374.

(59) Showell, G. A.; Baker, R.; Davis, J.; Hargreaves, R.; Freedman, S. B.; Hoogsteen, K.; Patel, S.; Snow, R. J. Synthesis and in Vitro Biological Profile of All Four Isomers of the Potent Muscarinic Agonist 3-(3-Methyl-1,2,4-oxadiazol-5-yl)-1-azabicyclo[2.2.1]-heptane. *J. Med. Chem.* **1992**, *35*, 911–916.

(60) Miller, D. D.; Harrold, M.; Wallace, R. A.; Wallace, L. J.; Uretsky, N. J. Dopaminergic Drugs in the Cationic Form Interact with D_2 Dopamine Receptors. *Trends Pharmacol. Sci.* **1988**, *9*, 282–284.

(61) NMR spectral properties: (a) Furans and benzofurans, see ref 35. (b) Thiophenes and benzothiophenes, see: Kellogg, R. M. In *Comprehensive Heterocyclic Chemistry*; Katritzky, A. R., Rees, C. W., Eds.; Pergamon Press: Oxford, 1984; Vol. 4, pp 713–740 and references cited therein. (c) Selenophenes, see: Bird, C. W.; Cheeseman, G. W.; Hörnfeldt, A.-B. In *Comprehensive Heterocyclic Chemistry*; Katritzky, A. R., Rees, C. W., Eds.; Pergamon Press: Oxford, 1984; Vol. 4, pp 935–971 and references cited therein.

(62) The ^{13}C NMR spectrum on the free base of **47** showed separate signals due to C6 and C7 (see the supplementary material).

(63) Chloroform was exchanged for dichloromethane in the chromatographic procedure since complete quaternization by *N*-chloromethylation occurred when the diastereomeric mixture was kept in a dichloromethane solution at room temperature overnight. A control experiment (see the Experimental Section) performed on **45b** confirmed the structure of the product (**46**).

46
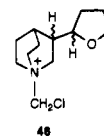
Compare: (a) Nevstad, G. O.; Songstad, J. Solvent Properties of Dichloromethane. II. The Reactivity of Dichloromethane Toward Amines. *Acta Chem. Scand.* **1984**, *B38*, 469–477. (b) Langlois, M.; Soulier, J. L.; Mathé-Allainmat, M.; Gallais, C.; Brémont, B.; Shen, S. *N*-Chloromethyl Quinuclidinium Derivatives: A New Class of Irreversible Ligands for 5-HT$_3$ Receptors. *Bioorg. Med. Chem. Lett.* **1994**, *4*, 945–948.

(64) The signals due to dihydrobenzofuran 2-CH were obscured by a solvent peak when the spectrum was recorded in CD_3OD.

(65) These signals are in part overlapping.

(66) Compare: Albert, A.; Serjeant, E. P. *The Determination of Ionization Constants*, 2nd ed.; Chapman and Hall Ltd: London, 1971.

(67) TRIPOS Associates, Inc., 1699 S. Hanley Road, Suite 303, St. Louis, MO 63144.

(68) Wavefunction Inc., 18401 Von Karman Avenue, Suite 370, Irvine, CA 92715.

(69) Lowry, O. H.; Rosebrough, N. J.; Far, A. L.; Randall, R. J. Protein Measurements with the Folin Phenol Reagent. *J. Biol. Chem.* **1951**, *193*, 265–275.

(70) Jacobs, S.; Chang, K.-J.; Cuatrecasas, P. Estimation of Hormone Receptor Affinity by Competitive Displacement of Labelled Ligand. Effects of Concentration of Receptor and Labelled Ligand. *Biochem. Biophys. Res. Commun.* **1975**, *66*, 687–692.

(71) Schild, H. I. pAx and Competitive Drug Antagonism. *Br. J. Pharmacol. Chemother.* **1949**, *4*, 277–280.

(72) Cherry, W. H.; Davies, W.; Ennis, B. C.; Porter, Q. N. The Base-Catalyzed Skeletal Rearrangement of a Thianaphthofluorene Derivative. *Aust. J. Chem.* **1967**, *20*, 313–320.

(73) Acheson, R. M.; Harrison, D. R. The Synthesis, Spectra, and Reactions of Some S-Alkylthiophenium Salts. *J. Chem. Soc. C* **1970**, 1764–1784.

(74) Geneste, P.; Olivé, J.-L.; Ung, S. N.; El Amoudi El Faghi, M.; Easton, J. W.; Beierbeck, H.; Saunders, J. K. Carbon-13 Nuclear Magnetic Resonance Study of Benzo[*b*]thiophenes and Benzo[*b*]thiophene S-Oxides and S,S-Dioxides. *J. Org. Chem.* **1979**, *44*, 2887–2892.

(75) See, e.g.: (a) Jutzi, P.; Gilge, U. Synthese von Benzoxazol-2-yl Trimethylsilan und -Stannan. (Synthesis of benzoxazol-2-yl-trimethylsilane and -stannane.) *J. Organomet. Chem.* **1983**, *246*, 159–162. (b) Moderhack, D.; Stolz, K. Cycloaddition von *N*-Aryl-*tert*-butylketeniminen an Nitrosobenzol sowie 2-Methyl-2-nitrosopropan. (Cycloaddition of N-aryl-*tert*-butylketenimines to both nitrosobenzene and 2-methyl-2-nitrosopropane.) *Chem. Ber.* **1986**, *119*, 3411–3421.

(76) Nilvebrant, L.; Sparf, B. Receptor Binding Profiles of Some Selective Muscarinic Antagonists. *Eur. J. Pharmacol.* **1988**, *151*, 83–96.